

# Diffusion Bridge Mixture Transports, Schrödinger Bridge Problems and Generative Modeling

Stefano Peluchetti  
Cogent Labs  
speluchetti@cogent.co.jp

## Abstract

The dynamic Schrödinger bridge problem seeks a stochastic process that defines a transport between two target probability measures, while optimally satisfying the criteria of being closest, in terms of Kullback-Leibler divergence, to a reference process. The classical algorithm utilized for solving this problem is the iterative proportional fitting procedure (IPF, [Ruschendorf \(1995\)](#)). Recent approaches for a diffusion reference process by [Bortoli et al. \(2021\)](#); [Vargas et al. \(2021\)](#) employ a time reversal argument to develop sampling-based implementations of the IPF procedure, which are shown to scale well in high-dimensional settings. A major shortcoming of the IPF procedure is that it achieves a valid coupling between the two target measures only when the number of iterations grows unbounded. Furthermore, sampling-based time reversal approaches suffer from a simulation-inference mismatch, which can adversely impact the performance of the resulting algorithm.

We propose a novel sampling-based iterative algorithm, the iterated diffusion bridge mixture transport (IDBM), aimed at solving the dynamic Schrödinger bridge problem. The IDBM procedure exhibits the attractive property of realizing a valid coupling between the target measures at each step. Additionally, each step of the IDBM procedure is by design not affected by simulation-inference mismatches. We perform an initial theoretical investigation of the IDBM procedure, establishing its convergence properties. The theoretical findings are complemented by numerous numerical experiments illustrating the competitive performance of the IDBM procedure across various applications.

Recent advancements in generative modeling also employ the time-reversal of a diffusion process to define a generative process that approximately transports a simple distribution to the data distribution ([Song et al., 2021](#)). As an alternative, we propose using the first iteration of the IDBM procedure as an approximation-free method for realizing this transport. This approach offers greater flexibility in selecting the generative process dynamics and exhibits faster training and superior sample quality over longer discretization intervals. In terms of implementation, the necessary modifications are minimally intrusive, being limited to the training loss computation, with no changes necessary for generative sampling.

## 1 Introduction

Generating samples from a given distribution is a central topic in computational statistics and machine learning. In recent years, transportation of probability measures has gained considerable attention as a computational tool for sampling. The underlying concept entails generating samples from a complex distribution by first obtaining samples from a simpler distribution, and subsequently computing a suitably constructed map of these samples

(El Moselhy and Marzouk, 2012; Marzouk et al., 2016). Let us consider the following definition: given two probability measures  $\Gamma$  and  $\Upsilon$ , a transport from  $\Gamma$  to  $\Upsilon$  is defined as a map  $h(X, \varepsilon)$ , where  $\varepsilon$  is an independent auxiliary random element, such that if  $X \sim \Gamma$  (i.e.,  $X$  is distributed according to  $\Gamma$ ), then  $Y = h(X, \varepsilon)$  satisfies  $Y \sim \Upsilon$ . This broad definition encompasses both deterministic and random transports and includes a wide range of sampling methods, such as Markov Chain Monte Carlo (Brooks et al., 2011), normalizing flows (Papamakarios et al., 2021), and score-based generative modeling (Song et al., 2021).

To narrow down the extensive class of possible transports, a potential approach involves identifying the optimal transport based on a suitably chosen criterion. This paper addresses a more generalized version of the optimization problem initially posed by Schrödinger in 1931 (Léonard, 2014b). In this context, both  $\Gamma$  and  $\Upsilon$  are defined on the same  $d$ -dimensional Euclidean space. The optimization space comprises  $d$ -dimensional diffusion processes on the time interval  $[0, \tau]$ , constrained to have initial distribution  $\Gamma$  and terminal distribution  $\Upsilon$ . Optimality is achieved minimizing the Kullback-Leibler divergence to a reference diffusion process. The optimal map  $Y = h(X, \varepsilon)$  is obtained by defining  $\varepsilon$  as the  $d$ -dimensional Brownian motion on  $[0, \tau]$  which drives the optimal diffusion process started at  $X$ , with terminal value  $Y$ . This seemingly intricate method of defining a transport is of practical relevance. When the reference diffusion is given by a scaled Brownian motion  $\sigma W_t$ , for some  $\sigma > 0$ ,  $(X, h(X, \varepsilon))$  solves the entropic regularized optimal transport (EOT) problem (Peyré and Cuturi, 2020, Chapter 4) for the regularization level  $2\sigma^2$ . EOT provides a more tractable alternative to solving the optimal transport (OT) problem. However, in high-dimensional settings, solving the EOT problem remains challenging. The dynamic formulation, achieved by inflating the original space where  $\Gamma$  and  $\Upsilon$  are supported so that they correspond to the initial-terminal distributions of a stochastic process, is essential to recent computational advancements in these demanding settings. Specifically, Bortoli et al. (2021); Vargas et al. (2021) rely on a time-reversal result for diffusion processes to implement sample-based iterative algorithms aimed at solving the dynamic Schrödinger bridge problem.

## 1.1 Our Contributions

In this work, we begin by reviewing the theory of Schrödinger bridge problems in their various forms, as well as the approaches presented by Bortoli et al. (2021); Vargas et al. (2021). We establish that sample-based time-reversal approaches suffer from a simulation-inference mismatch. Specifically, at each iteration, samples from the previous iteration are utilized to infer a new diffusion process, but relevant regions of the state space can be left unexplored. This issue is particularly prominent in scenarios characterized by a low level of randomness in the reference process. This is problematic when the goal is to solve the OT problem: for the EOT solution to closely approximate the OT solution,  $\sigma$  must be small.

The primary contribution of this work is the development of a novel sample-based iterative algorithm, the IDBM procedure, for addressing the dynamic Schrödinger bridge problem. We begin by noting that the problem’s solution, i.e. the optimal diffusion process, can be represented as a mixture of diffusion bridges, with the mixing occurring over the bridges’ initial-terminal distributions. In general, processes constructed in this manner are not diffusion processes (Jamison, 1974, 1975). The IDBM procedure involves the following iterative steps: (i) constructing a stochastic process as a mixture of diffusion bridges such that its initial-terminal distribution forms a coupling of the target probability measures  $\Gamma$  and  $\Upsilon$ ; (ii) matching the marginal distributions of the stochastic process generated in (i) with a diffusion process; (iii) updating the coupling from step (i) with the initial-terminal distributions of the diffusion

obtained in step (ii). The drift of the diffusions process of step (ii) is inferred based on samples from the stochastic process of step (i). Crucially, as both processes share the same marginal distributions, no simulation-inference mismatch occurs. In this study, we conduct an initial theoretical examination of the IDBM procedure, establishing its convergence in law towards the solution to the dynamic Schrödinger bridge problem. Additionally, we carry out empirical evaluations of the IDBM procedure in comparison to the IPF procedure, highlighting its robustness properties.

The recent advancements in score-based generative approaches (Song et al., 2021; Rombach et al., 2022) have demonstrated remarkable generative quality in visual applications by leveraging the time-reversal of a diffusion process to define the sampling process. To elaborate further, the reference diffusion’s dynamics are selected based on a decoupling criterion, which requires the process’s terminal value to be approximately independent of the process’s initial value. The reference process’s initial distribution is assumed to be the empirical distribution of a dataset of interest, or a slightly perturbed version of it. The time reversal of the reference diffusion, complemented by a dataset-independent initial distribution, defines the sampling process. In this work, we propose to utilize the first iteration of the IDBM procedure as an alternative method of defining a sampling process targeting a dataset of interest. Under this proposal, the reference diffusion’s dynamics are no longer constrained by decoupling considerations. We conduct an empirical evaluation of the resulting transport, demonstrating its competitiveness for visual applications in comparison to the approach of Song et al. (2021). Remarkably, the proposed approach displays accelerated training and superior sample quality at larger discretization intervals without fine-tuning the involved hyperparameters. From a practitioner standpoint, implementing the proposed method requires minimal changes, which are confined to the computation of the training loss function.

## 1.2 Structure of the Paper

The paper is structured as follows. In Section 2 we introduce the Schrödinger bridge problem in its various forms, the IPF procedure, its time-reversal sample-based implementations for the case of a reference diffusion process, and score-based generative modeling. The IDBM transport, its convergence properties, and suitable training objectives are presented in Section 3. In Section 4 we define the class of reference SDEs considered in the applications discussed in Section 5. Section 6 provides concluding remarks for the paper. Proofs, auxiliary formulae, code listings and a table summarizing the notation used throughout this work are deferred to the Appendices.

## 1.3 Notation and Preliminaries

In light of the methodological focus of the present work, we refrain from discussing some of the more technical aspects. The excellent treatises by Léonard (2014b,a) provide a formal account of the preliminaries discussed in this section and of the developments of Section 2.1. To aid the reader, a summary of the main notation is provided in Table 2 in Appendix D.

All stochastic processes we are concerned with are defined over the continuous time interval  $[0, \tau]$ , have state space  $\mathbb{R}^d$ , and are continuous, for some constants  $\tau > 0$  and  $d \geq 1$ . A realization of a stochastic process, or path, is an element  $x \in \mathcal{C}([0, \tau], \mathbb{R}^d)$ , the space of continuous functions from  $[0, \tau]$  to  $\mathbb{R}^d$ .

We denote each probability measure (PM) with an uppercase letter. For a PM  $P$ ,  $X \sim P$  denotes that  $X$  is a random element with distribution  $P$ . Let  $n \geq 1$  and  $t_1, \dots, t_n \in [0, \tau]$ .

We denote the collection of PMs over  $\mathcal{C}([0, \tau], \mathbb{R}^d)$  with  $\mathcal{P}_{\mathcal{C}}$  and the collection of PMs over  $\mathbb{R}^{d \times n}$  with  $\mathcal{P}_n$ . When  $P \in \mathcal{P}_n$  admits a density with respect to the Lebesgue measure on  $\mathbb{R}^{d \times n}$  we denote this density with the same lowercase letter (here  $p$ ). For  $P \in \mathcal{P}_{\mathcal{C}}$ , we denote with  $P_{t_1, \dots, t_n} \in \mathcal{P}_n$  the marginalization of  $P$  at  $t_1, \dots, t_n$  and with  $P_{\bullet|t_1, \dots, t_n} \in \mathcal{P}_{\mathcal{C}}$  the conditioning of  $P$  given the values at times  $t_1, \dots, t_n$ . More explicitly, if  $X \sim P \in \mathcal{P}_{\mathcal{C}}$ , we have  $P_{t_1, \dots, t_n}(A_1, \dots, A_n) = \Pr[X_{t_1} \in A_1, \dots, X_{t_n} \in A_n]$  and  $P_{\bullet|t_1, \dots, t_n}(A|x_1, \dots, x_n) = \Pr[X \in A | X_{t_1} = x_1, \dots, X_{t_n} = x_n]$ . A path PM can be defined via a mixture: if  $\Psi \in \mathcal{P}_n$  and  $P \in \mathcal{P}_{\mathcal{C}}$ , let  $Q = \Psi P_{\bullet|t_1, \dots, t_n}$  stand for  $Q(A) = \int P_{\bullet|t_1, \dots, t_n}(A|x_1, \dots, x_n) \Psi(dx_1, \dots, dx_n)$ . That is,  $Q$  is obtained by pinning down  $X \sim P$  at times  $t_1, \dots, t_n$ , and taking a mixture with respect to  $\Psi$  over the pinned down values. With this notation, the marginal-conditional decomposition of  $P \in \mathcal{P}_{\mathcal{C}}$  is  $P = P_{t_1, \dots, t_n} P_{\bullet|t_1, \dots, t_n}$ . If  $P, Q \in \mathcal{P}_{\mathcal{C}}$ , and  $P$  is absolutely continuous with respect to  $Q$  ( $P \ll Q$ ) with density  $(dP/dQ)(x)$ , the marginal-conditional decomposition of  $(dP/dQ)(x)$  is  $(dP/dQ)(x) = (dP_{t_1, \dots, t_n}/dQ_{t_1, \dots, t_n})(x_{t_1}, \dots, x_{t_n}) \times (dP_{\bullet|t_1, \dots, t_n}/dQ_{\bullet|t_1, \dots, t_n})(x)$ . For two PMs  $P$  and  $Q$ ,  $P \sim Q$  denotes that  $P$  and  $Q$  are equivalent PMs (they share the same null sets).

Given two PMs  $\Gamma, \Upsilon \in \mathcal{P}_1$ , we define  $\mathcal{P}_{\mathcal{C}}(\Gamma, \Upsilon) \subseteq \mathcal{P}_{\mathcal{C}}$  as the collection of PMs having  $\Gamma$  as initial distribution and  $\Upsilon$  as terminal distribution. Hence,  $P \in \mathcal{P}_{\mathcal{C}}(\Gamma, \Upsilon)$  transports  $\Gamma$  to  $\Upsilon$ :  $P_0 = \Gamma, P_{\tau} = \Upsilon$ , while its time reversal transports  $\Upsilon$  to  $\Gamma$ . We write  $\mathcal{P}_{\mathcal{C}}(\Gamma, \cdot)$  when only the initial distribution is fixed, and  $\mathcal{P}_{\mathcal{C}}(\cdot, \Upsilon)$  when only the terminal distribution is fixed. We define  $\mathcal{P}_2(\Gamma, \Upsilon) \subseteq \mathcal{P}_2$  as the collection of PMs with prescribed marginal distributions  $\Gamma$  and  $\Upsilon$ , i.e. the collection of couplings between  $\Gamma$  and  $\Upsilon$ . We write  $\mathcal{P}_2(\Gamma, \cdot)$  ( $\mathcal{P}_2(\cdot, \Upsilon)$ ) when only the first (second) marginal distribution is fixed. For  $P \in \mathcal{P}_2$ , we write  $P_0, P_{\tau}$  to denote respectively the first and second marginal, and denote the conditional distributions with  $P_{\bullet|0}$  and  $P_{\bullet|\tau}$ . With this notation, for  $P \in \mathcal{P}_{\mathcal{C}} \cup \mathcal{P}_2$  we have  $P = P_0 P_{\bullet|0} = P_{\tau} P_{\bullet|\tau}$ .

We write  $\mathcal{U}(0, \tau)$  for the uniform distribution on  $(0, \tau)$ ,  $\mathcal{N}_d(\mu, \Sigma)$  for the  $d$ -variate normal distribution with mean  $\mu \in \mathbb{R}^d$  and covariance  $\Sigma \in \mathbb{R}^d \times \mathbb{R}^d$ . For  $S, R$  two PMs on the same space, the Kullback-Leibler (KL) divergence from  $S$  to  $R$  is defined as  $D_{KL}(S \| R) := \mathbb{E}_S[\log(\frac{dS}{dR})]$  whenever  $S \ll R$ ,  $+\infty$  otherwise.

We denote identity matrices with  $I$ , and transposition of a square matrix  $A$  with  $A^{\top}$ . We use the notation  $[A]_i$  and  $[A]_{i,j}$  to denote indexing respectively of a vector and of a matrix. The Euclidean norm of a vector  $V$  is denoted by  $\|V\|$ .

If  $X \sim P \in \mathcal{P}_{\mathcal{C}}$ , we denote the time reversal of  $X$  with  $\bar{X}$ , that is  $\bar{X}_t := X_{\tau-t}$  ( $t \in [0, \tau]$ ). The time reversal of  $P$  itself is defined as  $\bar{P}[A] := P[\bar{A}]$ ,  $\bar{A} := \{x : x_{\tau-t} \in A\}$ , so that  $\bar{X} \sim \bar{P}$ . Note that  $E_P[f(X)] = E_{\bar{P}}[f(\bar{X})]$  for any integrable  $f : \mathcal{C}([0, \tau], \mathbb{R}^d) \rightarrow \mathbb{R}$ . Thorough the paper we set  $\tau := \tau - t$ .

Without further mention, all SDE drift coefficients are assumed to be  $\mathbb{R}^d$ -valued and all SDE diffusion coefficients are assumed to be  $\mathbb{R}^d \times \mathbb{R}^d$ -valued. Most SDEs, and associated diffusion solutions, are denoted with the same letter  $X$ . To avoid ambiguity, we clearly denote the corresponding probability laws. Similarly, we denote most  $\mathbb{R}^d$ -valued standard Brownian motions with  $W$ . It is understood that all Brownian motions driving different SDEs are independent nonetheless.

## 2 Schrödinger Bridge Problems

In Section 2.1 we review the theory of Schrödinger bridge problems in both dynamic and static formulations. We initially consider the generic setting of continuous stochastic processes before specializing in the case of a diffusion reference measures. In Sections 2.2 and 2.3, we discuss

the classical iterative algorithm employed in the numerical solution to the Schrödinger bridge problems, focusing on recent contributions that rely on a time reversal argument for diffusion processes. Throughout our discussion, we adopt a path space, or continuous-time, perspective. This perspective not only provides clarity but also highlights the connection with a sequential estimation problem for diffusion processes. For the sake of completeness, we review the basics of simulation and inference for SDEs in Section 2.4. Finally, in Section 2.5, review score-based generative modeling, emphasizing its connections to the dynamic Schrödinger bridge problem.

## 2.1 Dynamic, Static and Half Versions

For  $\Gamma, \Upsilon \in \mathcal{P}_1$ ,  $R \in \mathcal{P}_C$ , the solution to the dynamic Schrödinger bridge problem ( $S_{\text{dyn}}$ ) is given by

$$S^*(\Gamma, \Upsilon, R, \mathcal{P}_C) := \arg \min_{S \in \mathcal{P}_C(\Gamma, \Upsilon)} D_{KL}(S \parallel R).$$

( $S_{\text{dyn}}$ ) seeks a stochastic process transporting an initial distribution  $\Gamma$  to a terminal distribution  $\Upsilon$ , while achieving minimum Kullback-Leibler (KL) divergence to the reference law  $R$ . For a given  $S \in \mathcal{P}_C$ ,  $S \ll R$ , the marginal-conditional decompositions for PMs and densities give

$$\begin{aligned} D_{KL}(S \parallel R) &= \mathbb{E}_{S_{0,\tau}} \left[ \mathbb{E}_{S_{\bullet|0,\tau}} \left[ \log \left( \frac{dS_{0,\tau}}{dR_{0,\tau}}(x_0, x_\tau) \frac{dS_{\bullet|0,\tau}}{dR_{\bullet|0,\tau}}(x) \right) \right] \right] \\ &= D_{KL}(S_{0,\tau} \parallel R_{0,\tau}) + \mathbb{E}_{S_{0,\tau}} [D_{KL}(S_{\bullet|0,\tau} \parallel R_{\bullet|0,\tau})]. \end{aligned} \quad (1)$$

The second term of (1) is minimized by  $S_{\bullet|0,\tau}^*(\Gamma, \Upsilon, R, \mathcal{P}_C) = R_{\bullet|0,\tau}$ , independently of  $\Gamma, \Upsilon$ , yielding the representation of  $S^*(\Gamma, \Upsilon, R, \mathcal{P}_C)$  as a mixture of the reference process pinned down at its initial and terminal values. The mixing distribution  $S_{0,\tau}^*(\Gamma, \Upsilon, R, \mathcal{P}_C)$  over the initial and terminal values minimizes the first term of (1), i.e. it solves a specific instance of the following problem.

For  $\Gamma, \Upsilon \in \mathcal{P}_1$ ,  $B \in \mathcal{P}_2$ , the solution to the static Schrödinger bridge problem ( $S_{\text{sta}}$ ) is given by

$$S^*(\Gamma, \Upsilon, B, \mathcal{P}_2) := \arg \min_{C \in \mathcal{P}_2(\Gamma, \Upsilon)} D_{KL}(C \parallel B).$$

( $S_{\text{sta}}$ ) differs from ( $S_{\text{dyn}}$ ) in the optimization space:  $\mathcal{P}_2$  instead of  $\mathcal{P}_C$ . With this notation,  $S_{0,\tau}^*(\Gamma, \Upsilon, R, \mathcal{P}_C) = S^*(\Gamma, \Upsilon, R_{0,\tau}, \mathcal{P}_2)$ , the solution to ( $S_{\text{sta}}$ ) for  $B = R_{0,\tau}$ . The solution to ( $S_{\text{dyn}}$ ) is then  $S^*(\Gamma, \Upsilon, R, \mathcal{P}_C) = S^*(\Gamma, \Upsilon, R_{0,\tau}, \mathcal{P}_2) R_{\bullet|0,\tau}$ . Vice versa, if  $S^*(\Gamma, \Upsilon, R, \mathcal{P}_C)$  solves ( $S_{\text{dyn}}$ ), then  $S_{0,\tau}^*(\Gamma, \Upsilon, R, \mathcal{P}_C)$  solves ( $S_{\text{sta}}$ ) for  $B = R_{0,\tau}$ . From this point onward, ( $S_{\text{sta}}$ ) is always understood to be associated to the corresponding ( $S_{\text{dyn}}$ ), i.e. we will only consider ( $S_{\text{sta}}$ ) for  $B = R_{0,\tau}$ . It established in [Rüschendorf and Thomsen \(1993\)](#) that, if there is a  $C \in \mathcal{P}_2(\Gamma, \Upsilon)$  such that  $D_{KL}(C \parallel R_{0,\tau}) < \infty$ , then ( $S_{\text{sta}}$ ) admits a solution, which is unique. This hypothesis is assumed to hold thorough the paper.

We introduce an additional axis among which to classify Schrödinger bridge problems, covering both dynamic ( $H_{\text{dyn}}$ ) and static ( $H_{\text{sta}}$ ) variants jointly for brevity. Thus, let  $\mathcal{P}$  be either  $\mathcal{P}_C$  (case of ( $H_{\text{dyn}}$ )) or  $\mathcal{P}_2$  (case of ( $H_{\text{sta}}$ )). For  $\Gamma, \Upsilon \in \mathcal{P}_1$ ,  $Q \in \mathcal{P}$ , the solutions to the forward and to the backward Schrödinger half bridge problems are respectively given by

$$\begin{aligned} S^*(\Gamma, \cdot, Q, \mathcal{P}) &:= \arg \min_{H \in \mathcal{P}(\Gamma, \cdot)} D_{KL}(H \parallel Q), \\ S^*(\cdot, \Upsilon, Q, \mathcal{P}) &:= \arg \min_{H \in \mathcal{P}(\cdot, \Upsilon)} D_{KL}(H \parallel Q). \end{aligned}$$

In contrast to  $(S_{\text{dyn}})$  and  $(S_{\text{sta}})$ , only one of the marginal conditions is enforced. The forward and backward half bridge problems admit simpler solutions which form the basis of the developments of Section 2.2. Proceeding as in (1), it can be established that for  $H \in \mathcal{P}$  such that  $H \ll Q$

$$\begin{aligned} D_{KL}(H \parallel Q) &= D_{KL}(H_0 \parallel Q_0) + \mathbb{E}_{H_0} [D_{KL}(H_{\bullet|0} \parallel Q_{\bullet|0})] \\ &= D_{KL}(H_\tau \parallel Q_\tau) + \mathbb{E}_{H_\tau} [D_{KL}(H_{\bullet|\tau} \parallel Q_{\bullet|\tau})], \end{aligned} \quad (2)$$

from which we obtain the half bridge solutions  $S^*(\Gamma, \cdot, Q, \mathcal{P}) = \Gamma Q_{\bullet|0}$  and  $S^*(\cdot, \Upsilon, Q, \mathcal{P}) = \Upsilon Q_{\bullet|\tau}$ . That is, one of the endpoint (or marginal, for  $(H_{\text{sta}})$ ) distributions of  $Q = Q_0 Q_{\bullet|0} = Q_\tau Q_{\bullet|\tau}$  is replaced by one of  $\Gamma, \Upsilon$  while keeping the associated conditional distribution of  $Q$  constant. In the case of  $(H_{\text{dyn}})$ , it thus suffices to propagate the initial (terminal) distribution  $\Gamma$  ( $\Upsilon$ ) through the forward (backward) dynamics of  $Q$ :  $Q_{\bullet|0}$  ( $Q_{\bullet|\tau}$ ).

$R_0$  plays a minor role in  $(S_{\text{dyn}})$ . From (2) applied with  $Q = R$ ,  $H \in \mathcal{P}_{\mathcal{C}}$ , either  $R_0$  is such that  $(S_{\text{dyn}})$  do not admit any solution (when  $D_{KL}(S \parallel R) = +\infty$  for every  $S \in \mathcal{P}_{\mathcal{C}}(\Gamma, \Upsilon)$ ), or the solution to  $(S_{\text{dyn}})$  exists, is unique, and is independent of  $R_0$ . This work is concerned with the case where  $R$  is given by the solution to a  $d$ -dimensional stochastic differential equation (SDE), i.e. a diffusion process (Øksendal, 2003; Friedman, 1975). We consider the following reference SDE, with initial distribution  $\Gamma$  (without loss of generality),

$$\begin{aligned} dX_t &= \mu_R(X_t, t)dt + \sigma_R(X_t, t)dW_t, \quad t \in [0, \tau], \\ X_0 &\sim \Gamma. \end{aligned} \quad (3)$$

Thorough the paper, it is assumed that (3) admits a unique (weak, non-explosive) solution, whose law defines the reference law  $R = \Gamma R_{\bullet|0}$ . It is also assumed that  $R \ll R^\circ$  where  $R^\circ$  is the law of the unique solution to (3) with  $\mu_R(x, t) = 0$ . These are mild assumptions. The law  $R_{\bullet|0}$  only depends on the drift coefficient  $f(x, t)$  and on the diffusion coefficient  $\sigma_R(x, t)$ . Here and in the following  $\Sigma_R(x, t) := \sigma_R(x, t)\sigma_R(x, t)^\top$  is assumed to be invertible.

## 2.2 Iterative Proportional Fitting (IPF)

The main tool employed in the numerical solution to  $(S_{\text{dyn}})$  and  $(S_{\text{sta}})$  is an iterative numerical procedure, known in the literature under a variety of names. In  $(S_{\text{sta}})$ , when  $\Gamma$  and  $\Upsilon$  are admits Lebesgue densities  $\gamma(\cdot)$  and  $\nu(\cdot)$  the term *Fortet iterations* (Fortet, 1940) is used. Instead, when  $\Gamma$  and  $\Upsilon$  concentrate all mass on a finite set of values, the term *iterative proportional fitting* procedure (Deming and Stephan, 1940) is used. In the same setting, due to an equivalence between  $(S_{\text{sta}})$  and entropy-regularized optimal transport (Peyré and Cuturi, 2020, Chapter 4), the same procedure is also known as *Sinkhorn algorithm*. Finally, the term IPF can also refer to the iterative solution to the measure-theoretic formulation of Ruschendorf (1995), including the dynamic version  $(S_{\text{dyn}})$  (Bernton et al., 2019). In this work, we use the IPF term.

For  $(S_{\text{sta}})$  or  $(S_{\text{dyn}})$ , the IPF procedure (Algorithm 1) is obtained by iteratively solving the forward and backward half bridge problems. More precisely, let  $\mathcal{P}$  be either  $\mathcal{P}_{\mathcal{C}}$  or  $\mathcal{P}_2$ ,  $R \in \mathcal{P}$ ,  $\Gamma, \Upsilon \in \mathcal{P}_1$ , and assume without loss of generality that  $R = \Gamma R_{\bullet|0}$ . The IPF procedure is defined by the iterates  $F^{(0)} = R = S^*(\Gamma, \cdot, R, \mathcal{P})$ ,  $F^{(1)} = S^*(\cdot, \Upsilon, F^{(0)}, \mathcal{P})$ ,  $F^{(2)} = S^*(\Gamma, \cdot, F^{(1)}, \mathcal{P})$ ,  $\dots$  Under appropriate conditions (Ruschendorf, 1995), the measures  $F^{(i)}$  associated to the IPF iterates of Algorithm 1 converge in total variation (TV) metric and in KL divergence to  $S^*(\Gamma, \Upsilon, R, \mathcal{P})$  as  $i \rightarrow \infty$ . Note that our choice of indexing of the IPF iterations differs

from the prior literature, where indexing starts from 1. In this work, indexing reflects the number of learning problems that needs to be solved in order to produce samples from the corresponding IPF iteration. As simulation from (3) is in general feasible (Section 2.4), and can be carried out exactly for the specifications of interest (Section 4), no learning is required to produce samples from  $F^{(0)}$ .

---

**Algorithm 1** IPF

---

**Input:**  $\Gamma, \Upsilon, R_{\bullet|0}, n$

**Output:**  $\{F^{(i)}\}_{i=0}^n$

```

1:  $F_{\bullet|0}^{(0)} \leftarrow R_{\bullet|0}$ 
2: for  $i = 1, \dots, n$  do
3:   if  $i$  is even then
4:      $F^{(i)} \leftarrow \Gamma F_{\bullet|0}^{(i-1)}$             $\triangleright$  forward IPF
5:   else
6:      $F^{(i)} \leftarrow \Upsilon F_{\bullet|\tau}^{(i-1)}$         $\triangleright$  backward IPF
7:   end if
8: end for

```

---

For  $(S_{\text{dyn}})$ , and specifically for the case of a reference diffusion law  $R$ , Bortoli et al. (2021); Vargas et al. (2021) introduce implementations of Algorithm 1 that rely on a time reversal result for diffusion processes (Anderson, 1982). Let  $X$  be the  $d$ -dimensional diffusion process with law  $P \in \mathcal{P}_{\mathcal{C}}$  arising as unique solution to the SDE

$$\begin{aligned} dX_t &= \mu(X_t, t)dt + \sigma_R(X_t, t)dW_t, \quad t \in [0, \tau], \\ X_0 &\sim P_0. \end{aligned} \tag{4}$$

Under suitable conditions, the time reversed process  $\bar{X}_t := X_{\tau-t}$  is still a diffusion process, arising as solution to the SDE

$$\begin{aligned} d\bar{X}_t &= v(\bar{X}_t, t)dt + \sigma_R(\bar{X}_t, \mathbf{r})dW_t, \quad t \in [0, \tau], \\ v(x, t) &:= -\mu(x, \mathbf{r}) + \nabla \cdot \Sigma_R(x, \mathbf{r}) + \Sigma_R(x, \mathbf{r}) \nabla_x \log p_{\mathbf{r}}(x), \\ \bar{X}_0 &\sim P_{\tau}. \end{aligned} \tag{5}$$

In (5)  $\mathbf{r} := \tau - t$ ,  $p_t(x)$  is the Lebesgue density of the marginal distribution  $P_t$ , and the  $d$ -dimensional vector  $\nabla \cdot \Sigma_R(x, t)$  is defined by  $[\nabla \cdot \Sigma_R(x, t)]_i := \sum_{j=1}^d \nabla_{x_j} [\Sigma_R(x, t)]_{i,j}$ ,  $1 \leq i \leq d$ . We refer to Haussmann and Pardoux (1986); Millet et al. (1989) for the conditions required on (4) for the time reversal (5) to hold.

### 2.3 Diffusion IPF as Iterative Simulation-Inference

Bortoli et al. (2021); Vargas et al. (2021) propose sampling-based implementations of Algorithm 1. At step  $i \geq 1$ , samples are generated from  $F^{(i-1)}$  to construct an approximation to  $F^{(i)}$ . This approximation is used in turn to generate samples from  $F^{(i)}$ , which form the input to step  $i + 1$ .

Let  $F^{(i-1)}$  be a diffusion associated to a SDE (which holds for  $i = 1$ , as  $F^{(0)} = R$ ). We show that  $F^{(i)}$  is also a diffusion associated to a different SDE. First, lines 4 and 6 of Algorithm 1 are modified respectively to  $F^{(i)} \leftarrow \Gamma \bar{F}_{\bullet|0}^{(i-1)}$  and  $F^{(i)} \leftarrow \Upsilon \bar{F}_{\bullet|0}^{(i-1)}$ . With this

choice, the path PMs associated to backward IPF steps are defined over a reverse (relatively to the forward IPF steps) timescale. Denote the drift and diffusion terms associated to  $F^{(i-1)}$  respectively with  $\mu_F^{(i-1)}(x, t)$  and  $\sigma_R(x, t)$ , so that  $\mu_F^{(0)}(x, t) = \mu_R(x, t)$ . It will become clear shortly why the diffusion coefficient is independent of  $i$ . If  $i$  is even, we have  $F_0^{(i)} = \Gamma$ , otherwise  $F_0^{(i)} = \Upsilon$ . Thus, for all  $i \geq 1$ ,  $F^{(i)} = F_0^{(i)} \overline{F}_{\bullet|0}^{(i-1)}$ . Crucially, from the time reversal result of [Anderson \(1982\)](#), we know that  $\overline{F}^{(i-1)}$  is the law of the diffusion associated to

$$\begin{aligned} d\overline{X}_t^{(i-1)} &= \mu_F^{(i)}(\overline{X}_t^{(i-1)}, t)dt + \sigma_R(\overline{X}_t^{(i-1)}, \mathbf{r})dW_t, \quad t \in [0, \tau], \\ \mu_F^{(i)}(x, t) &:= -\mu_F^{(i-1)}(x, \mathbf{r}) + \nabla \cdot \Sigma_R(x, \mathbf{r}) + \Sigma_R(x, \mathbf{r}) \nabla_x \log f_{\mathbf{r}}^{(i-1)}(x), \\ \overline{X}_0^{(i-1)} &\sim F_{\tau}^{(i-1)}. \end{aligned} \quad (6)$$

Moreover,  $\overline{F}^{(i-1)} = \overline{F}_{\tau}^{(i-1)} \overline{F}_{\bullet|0}^{(i-1)}$  and  $F^{(i)} = F_0^{(i)} \overline{F}_{\bullet|0}^{(i-1)}$  differs only in the initial distribution:  $F^{(i)}$  is associated to (6) with initial distribution  $F_0^{(i)}$ . An ideal implementation would thus iteratively compute the drift terms  $v^{(i)}(x, t)$  from  $F^{(i-1)}$  for all  $i \geq 1$ .

It is known that the convergence of the IPF iterations becomes problematic in the small noise regime ([Dvurechensky et al., 2018](#)), i.e. for a vanishing diffusion coefficient  $\sigma_R(x, t)$ . The aforementioned theoretical construction of the IPF iterations provides some insight. Consider  $F^{(0)}$ , solution to (3). Under appropriate conditions ([Stroock and Varadhan, 2006](#), Chapter 11), if  $\sigma_R(x, t)$  vanishes, the solution to (3) converges to the solution to the random ODE

$$\begin{aligned} dX_t &= \mu_R(X_t, t)dt, \quad t \in [0, \tau], \\ X_0 &\sim \Gamma. \end{aligned} \quad (7)$$

The time reversal of (7) is

$$\begin{aligned} d\overline{X}_t &= -\mu_R(\overline{X}_t, \mathbf{r})dt, \quad t \in [0, \tau], \\ \overline{X}_0 &\sim R_{\tau}, \end{aligned} \quad (8)$$

and  $F^{(1)}$  is the solution to (8) with  $\overline{X}_0 \sim \Upsilon$ . But  $F^{(2)}$  is given once again by the solution to (7), and the IPF iterations fail to converge. The key issue is the disappearance of the  $x$ -score  $\nabla_x \log f_{\mathbf{r}}^{(i-1)}(x)$  factor from (6), through which the laws of the IPF iterations propagate.

In practice, approximators  $\alpha_F^{(i)}(x, t) \approx \mu_F^{(i)}(x, t)$  are required. Relying directly on the functional form of the drifts  $\mu_F^{(i)}(x, t)$  forms the basis of the approach of Section 2.5, which is limited to  $i = 1$ . For  $i > 1$  scalability issues arise, as the nested application of (6) results in  $i$  approximators being employed at step  $i$ . Thus, [Bortoli et al. \(2021\)](#); [Vargas et al. \(2021\)](#) propose to directly infer the drift terms  $\mu_F^{(i)}(x, t)$  as  $F^{(i)}$  is the law of a diffusion process with known diffusion coefficient for every  $i \geq 0$ . The approach relies on two observations. First, generating a sample  $\overline{X}^{(i-1)} \sim \overline{F}^{(i-1)}$  is trivial if we have access to a sample  $X^{(i-1)} \sim F^{(i-1)}$ , as  $\overline{X}_t^{(i-1)} = X_{\tau-t}^{(i-1)}$ . Second, samples from  $\overline{F}^{(i-1)}$  suffice to carry out inference for  $F^{(i)}$ . Indeed,  $\overline{F}^{(i-1)}$  and  $F^{(i)}$  differing only in the initial distribution, are associated to the same SDE as previously remarked. These considerations suggest the following strategy: (i) use samples from  $\overline{F}^{(i-1)}$  to infer an approximator  $\alpha_F^{(i)}(x, t) \approx \mu_F^{(i)}(x, t)$ ; (ii) construct the SDE

$$\begin{aligned} dX_t^{(i)} &= \alpha_F^{(i)}(X_t^{(i)}, t)dt + \sigma_R(X_t^{(i)}, \mathbf{r})dW_t, \quad t \in [0, \tau], \\ X_0^{(i)} &\sim F_0^{(i)}, \end{aligned} \quad (9)$$

whose solution is approximately distributed as  $F^{(i)}$ . Samples from (9) are used in turn as input to step  $i + 1$ . After  $n$  steps a sequence of inferred drift terms  $\alpha_F^{(1)}(x, t), \dots, \alpha_F^{(n)}(x, t)$  is obtained.

A number of approximations are involved in the aforementioned approach. First, the simulation from each SDE (9) results in a discretization error. Second, the inferred drift terms  $\alpha_F^{(i)}(x, t)$ , differing from their ideal counterparts, give rise to an approximation error. The approximation error arises from the finite amount of data simulated from  $\bar{F}^{(i-1)}$  (Monte Carlo error), from the finite model capacity of an approximator  $\alpha_F^{(i)}(x, t) \approx \mu_F^{(i)}(x, t)$ , and from local minima in the optimization required to carry out inference. Both discretization and approximation errors can be well controlled by increasing the required computation effort.

However, at a more fundamental level, inference for  $\alpha_F^{(i)}(x, t)$  is based on samples from  $\bar{F}^{(i-1)}$ . As such we can expect a good approximation of  $\alpha_F^{(i)}(x, t)$  over the regions the path space  $\mathbb{R}^d \times [0, \tau]$  with non-negligible probability under  $\bar{F}^{(i-1)}$ . As noted,  $\bar{F}^{(i-1)}$  differs from  $F^{(i)}$  in its initial distribution, because in general  $F_0^{(i)} \neq \bar{F}_\tau^{(i-1)}$ . The equality holds at convergence ( $i \rightarrow \infty$ ) or when  $F_\tau^{(0)} = R_\tau = \Upsilon$ , in which case the problem to be solved is trivial:  $S^*(\Gamma, \Upsilon, R, \mathcal{P}) = R$ . Due to the mismatch between  $\bar{F}^{(i-1)}$  and  $F^{(i)}$ , it is possible for the simulated solution to (9) to explore regions of the path space with negligible probability under  $\bar{F}^{(i-1)}$ , where essentially no information has been available about the value of  $\mu_F^{(i)}(X_t, t)$  to be estimated. In Section 5.2 we show that, far from being just a theoretical concern, the simulation-inference distribution mismatch can have a concrete detrimental effect. Our proposal, introduced in Section 3, does not suffer from the aforementioned issue.

## 2.4 Inference and Simulation of SDEs

We now briefly turn our attention to the two unresolved issues: how to simulate paths from a SDE and how to perform inference for a diffusion process. For both these purposes, consider SDE (4) with corresponding diffusion solution  $P$ . Sample paths can be generated with arbitrary accuracy via a variety of discretization schemes, the simplest of which is the Euler scheme. Given a number of time steps  $m \geq 1$ , corresponding to a time increment  $\Delta t = \tau/m$ , a path discretization  $Y$  starting at  $Y_0 \sim P_0$  is generated sequentially on the time grid  $\{0, \Delta t, \dots, \tau\}$  as

$$Y_{t+\Delta t} = Y_t + \mu(Y_t, t)\Delta t + \sigma_R(Y_t, t)(W_{t+\Delta t} - W_t), \quad (W_{t+\Delta t} - W_t) \stackrel{\text{iid}}{\sim} \mathcal{N}_d(0, \Delta t I). \quad (10)$$

Convergence of discretization schemes can be assessed according to different metrics. Strong, or path-wise, convergence requires  $E[\|X_\tau - Y_\tau\|] \rightarrow 0$  as  $\Delta t \rightarrow 0$ , where  $X \sim P$  and the same Brownian motion  $W$  is driving both  $X$  and its discretization  $Y$ . More appropriate to our setting, weak convergence requires  $|E[f(X_\tau) - f(Y_\tau)]| \rightarrow 0$  as  $\Delta t \rightarrow 0$  for  $f(x) : \mathbb{R}^d \rightarrow \mathbb{R}$  belonging to a class of test functions. Kloeden and Platen (1992) contains a thorough coverage of discretization schemes for SDEs and of their convergence properties.

Inference for diffusion processes is a rich research area with long historical developments. We review only two basic approaches and refer to Hurn et al. (2007); Kessler et al. (2012); Fuchs (2013) and references therein for a broader overview. The key difficulty in performing maximum likelihood inference is that transition densities are seldom analytically available outside of restrictive SDEs' families. Discrete time series data can be observed at arbitrary long time intervals, and simple approximations (such as (10)) are accurate only on short time

intervals. In this sense, our setting simplifies inference: an arbitrary amount of data can be simulated at arbitrarily high frequency. Moreover, only the drift coefficient needs to be inferred.

Let  $Q \in \mathcal{P}_{\mathcal{C}}$  correspond to the solution to (4) for a different drift term  $\gamma(x, t)$ . Under suitable conditions, the Cameron-Martin-Girsanov formula provides the density between  $P_{\bullet|0}$  and  $Q_{\bullet|0}$  (Liptser and Shiriaev, 1977, Chapter 7),

$$\frac{dP_{\bullet|0}}{dQ_{\bullet|0}}(x) = \exp \left\{ \int_0^\tau [(\mu - \gamma)^\top \Sigma_R^{-1}](x_t, t) dx_t - \frac{1}{2} \int_0^\tau [(\mu - \gamma)^\top \Sigma_R^{-1}(\mu + \gamma)](x_t, t) dt \right\}. \quad (11)$$

In the following, let  $\alpha(x, t)$  be an approximating function for the drift coefficient  $\mu(x, t)$ . Maximum likelihood inference for  $\mu$  can be implemented with a driftless SDE acting as dominating measure  $P^*$ :

$$\mu(x, t) = \arg \max_{\alpha(x, t)} \mathbb{O}_{\text{MLE}}(\alpha, P), \quad \mathbb{O}_{\text{MLE}}(\alpha, P) := \mathbb{E}_P \left[ \frac{dP_{\bullet|0}}{dP^*_{\bullet|0}}(X) \right]. \quad (12)$$

The integrals in (11) need to be discretized, but the discretization errors can be controlled by simulating data at increasing frequencies.

An alternative approach is to consider one of the defining properties of diffusions, i.e. (Friedman, 1975, Chapter 5.4)

$$\mu(x, t) = \lim_{\Delta t \rightarrow 0^+} \frac{\mathbb{E}_P[X_{t+\Delta t} - X_t | X_t = x]}{\Delta t} \approx \mathbb{E}_P \left[ \frac{X_{t+\Delta t} - X_t}{\Delta t} \mid X_t = x \right]$$

for suitably small  $\Delta t$ , hence

$$\begin{aligned} \mu(x, t) &\approx \arg \min_{\alpha(x, t)} \mathbb{L}_{\text{DM}}(\alpha, P, \Delta t), \\ \mathbb{L}_{\text{DM}}(\alpha, P, \Delta t) &:= \mathbb{E}_{t \sim \mathcal{U}(0, \tau)} \left[ \mathbb{E}_P \left[ \left\| \alpha(X_t, t) - \frac{X_{t+\Delta t} - X_t}{\Delta t} \right\|^2 \right] \right], \end{aligned} \quad (13)$$

which matches the drift estimator derived in Bortoli et al. (2021).

## 2.5 Score-based Generative Modeling (SGM)

The approach of Song et al. (2021) is simpler, and corresponds to computing  $F^{(1)}$  in Algorithm 2, i.e. the time reversal of (3). SDE (3) is chosen to ensure approximate conditional independence of  $X_\tau$  from  $X_0$ , such that  $X_\tau \sim R_\tau \approx \Upsilon$  for a simple distribution  $\Upsilon$ . For a dataset of interest, the distribution of  $X_0$  is a smoothed version of the training data distribution, i.e.  $D_\eta := \frac{1}{n} \sum_{s=1}^n \mathcal{N}_d(x_s; 0, \eta^2 I_d) \in \mathcal{P}_1$  for a small scalar  $\eta \geq 0$  where  $\{x_s\}_{s=1}^n$  are the  $n$   $d$ -dimensional samples.  $\eta = 0$  corresponds to the empirical data distribution:  $D_0 = \frac{1}{n} \sum_{s=1}^n \delta_{x_s}$ . As observed in Section 2.3, due to the (approximate) decoupling of  $X_\tau$  from  $X_0$ ,  $F^{(0)}$  approximately solves (S<sub>dyn</sub>),  $F^{(0)} = R \approx S^*(D_\eta, \Upsilon, R, \mathcal{P}_{\mathcal{C}})$ , and  $F^{(1)}$  amounts to computing its time reversal. This also implies that, for specifications of (3) such that  $X_\tau$  is almost independent of  $X_0$ , there is no advantage in considering further IPF iterations.

In Song et al. (2021) an inferential procedure for computing the time reversal  $\bar{X}$  of (3) (detailed below) is developed and carried out, and  $\bar{X}_\tau$  is simulated to produce samples with distribution close to  $D_\eta$ . As shown in Section 4, a shortcoming of this approach is that achieving the decoupling of  $X_\tau$  from  $X_0$  corresponds to a large effective integration times,

rendering generation either computationally intensive or inaccurate. More precisely, the specification of (3) introduced in Song et al. (2021) for the CIFAR-10 datasets amounts to simulating a simpler SDE on the time interval  $[0, 50]$ , see Section 5.3. In turn, 1000 time steps (of an ad-hoc predictor-corrector discretization scheme) are employed for the simulation of  $\overline{X}_\tau$  to maximize the samples' visual quality.

Even though the inference techniques of Section 2.3 could also be applied to infer  $\overline{X}$ , SGM approaches leverage the specific form of the time reversal drift of (6), with the aim of learning the  $x$ -score  $\nabla_x \log r_t(x)$ . Inference is based on the minimization of a scalable version of the  $x$ -score matching objective (Hyvärinen, 2005), i.e. the left-hand side of

$$\mathbb{L}_{\text{SM}}(\alpha, R, t) := \mathbb{E}_R[\|\alpha(X_t, t) - \nabla_{X_t} \log r_{t|0}(X_t|X_0)\|^2] = \mathbb{E}_R[\|\alpha(X_t, t) - \nabla_{X_t} \log r_t(X_t)\|^2] + c,$$

where  $\alpha(x, t) : \mathbb{R}^d \times [0, \tau] \rightarrow \mathbb{R}^d$  is function approximating  $\nabla_x \log r_t(x)$  and  $c$  is independent of  $\alpha$ . The equality, which established in Vincent (2011), holds thanks to the mixture representation of  $R_{0,t}$ . While computing  $\nabla_x \log r_t(x)$  has computational cost  $\mathcal{O}(n)$ , which is impractical for large datasets, computing  $\nabla_x \log r_{t|0}(x|y)$  is  $\mathcal{O}(1)$  with respect to  $n$ . We provide a simpler derivation:

$$\begin{aligned} \nabla_{x_t} \log r_t(x_t) &= \frac{\nabla_{x_t} \int r_{t|0}(x_t|x_0) R_0(dx_0)}{r_t(x_t)} = \int \nabla_{x_t} \log r_{t|0}(x_t|x_0) \frac{r_{t|0}(x_t|x_0)}{r_t(x_t)} R_0(dx_0) \\ &= \mathbb{E}_R[\nabla_{X_t} \log r_{t|0}(X_t|X_0) | X_t = x_t], \end{aligned} \quad (14)$$

and by the projection property of conditional expectations,

$$\nabla_x \log r_t(x) = \arg \min_{\alpha(x,t)} \mathbb{E}_R[\|\alpha(X_t, t) - \nabla_{X_t} \log r_{t|0}(X_t|X_0)\|^2].$$

Both our derivation and the one of Vincent (2011) rely on exchange of limits which trivially hold when  $R_0 = D_\eta$ . In order to infer  $\nabla_x \log r_t(x)$  over all  $t \in [0, \tau]$ , the following objective is considered in Song et al. (2021)

$$\mathbb{L}_{\text{SM}}(\alpha, R) = \mathbb{E}_{t \sim \mathcal{U}(0, \tau)} [\lambda_t \mathbb{L}_{\text{SM}}(\alpha, R, t)],$$

where  $\lambda_t : (0, \tau) \rightarrow \mathbb{R}_{>0}$  is a time-dependent regularizer. Indeed, the conditional  $x$ -scores  $\nabla_x \log r_{t|0}(x|y)$  diverge as  $t \rightarrow 0$  (always, contrary to the  $x$ -score  $\nabla_x \log r_t(x)$  whose behavior for  $t \rightarrow 0$  is governed by  $R_0$ ), and it is sensible to normalize the orders of magnitude of  $\mathbb{L}_{\text{SM}}(\alpha, t)$  over the range of  $t$ .

Due to the identity (14), the generative process can be represented as

$$\begin{aligned} d\overline{X}_t &= \mu_F^{(1)}(\overline{X}_t, t) dt + \sigma_R(\overline{X}_t, \mathbf{r}) dW_t, \quad t \in [0, \tau], \\ \mu_F^{(1)}(x, t) &= -\mu_R(x, \mathbf{r}) + \nabla \cdot \Sigma_R(x, \mathbf{r}) + \Sigma_R(x, \mathbf{r}) \mathbb{E}_R[\nabla_{\overline{X}_t} \log r_{\mathbf{r}|0}(\overline{X}_t | \overline{X}_\tau) | \overline{X}_t = x], \\ \overline{X}_0 &\sim \Upsilon. \end{aligned} \quad (15)$$

In Song et al. (2021) a neural network  $\alpha_\theta(x, t)$  parametrized by  $\theta$  is employed as approximating function  $\alpha(x, t)$ . Having obtained an approximation  $\alpha_\theta(x, t) \approx \nabla_x \log r_t(x)$ , generation is achieved by numerically integrating (15) with  $\alpha_\theta(x, \mathbf{r})$  in place of  $\mathbb{E}_R[\nabla_{\overline{X}_t} \log r_{\mathbf{r}|0}(\overline{X}_t | \overline{X}_\tau) | \overline{X}_t = x]$  to sample  $\overline{X}_\tau$ .

### 3 Diffusion Bridge Mixture Transport

In this section we introduce a novel iterative algorithm for seeking the solution to  $(S_{\text{dyn}})$ . In Section 2.1, it is demonstrated that the solution to  $(S_{\text{dyn}})$  admits the representation  $S^*(\Gamma, \Upsilon, R, \mathcal{P}_C) = S^*(\Gamma, \Upsilon, R_{0,\tau}, \mathcal{P}_2)R_{\bullet|0,\tau}$ . We are concerned with the case where  $R$  corresponds to the diffusion process solution to (3), and in Section 3.1 we characterize  $R_{\bullet|0,\tau}$  as the law of a diffusion bridge. Considering the class of processes  $CR_{\bullet|0,\tau}$ , indexed by  $C \in \mathcal{P}_2(\Gamma, \Upsilon)$ , offers a natural means of approximating  $S^*(\Gamma, \Upsilon, R, \mathcal{P}_C)$ . At the same time, it is advantageous to exploit the dynamic nature of  $(S_{\text{dyn}})$ , rather than attempting to directly solve the  $(S_{\text{sta}})$  problem, by constructing a sequence of diffusion approximations to  $S^*(\Gamma, \Upsilon, R, \mathcal{P}_C)$ , as in Section 2.3. Processes formulated as  $CR_{\bullet|0,\tau}$  are investigated in Jamison (1974, 1975). In these studies (Section 3.2), it is revealed that  $CR_{\bullet|0,\tau}$  constitutes a diffusion process if and only if  $C = S^*(\Gamma, \Upsilon, R_{0,\tau}, \mathcal{P}_2)$ , which occurs at the optimum of  $(S_{\text{dyn}})$ . To circumvent this central issue, we draw upon a result that enables the construction of a diffusion process matching the marginal distribution of a mixture of diffusion processes (Section 3.3), of which  $CR_{\bullet|0,\tau}$  is a special case. The resulting transport is elaborated upon in Section 3.4, where we establish that its iterative application, the IDBM procedure, converges in law to  $S^*(\Gamma, \Upsilon, R, \mathcal{P}_C)$ . Each step of the IDBM procedure can be implemented both in forward and backward time. In Section 3.4, we present suitable inference objectives that enable sample-based implementations of the IDBM procedure.

#### 3.1 Diffusion Bridges

Consider (3) with initial value  $x_0$ , i.e.  $R_0 = \delta_{x_0}$ . Probabilistically conditioning (3) on hitting a terminal value  $x_\tau$  at time  $\tau$  results in the following SDE<sup>1</sup> with initial value  $x_0$  and terminal value  $x_\tau$  (Särkkä and Solin, 2019, Theorem 7.11)

$$\begin{aligned} dX_t &= b_R(X_t, t)dt + \sigma_R(X_t, t)dW_t, \quad t \in [0, \tau], \\ b_R(x, t) &:= \mu_R(x, t) + \Sigma_R(x, t) \nabla_x \log r_{\tau|t}(x_\tau|x), \\ X_0 &= x_0. \end{aligned} \tag{16}$$

The drift adjustment  $\Sigma_R(x, t) \nabla_x \log r_{\tau|t}(x_\tau|x)$  forces the process to hit  $x_\tau$  at time  $\tau$  and the diffusion process solving (16) is known as the diffusion bridge from  $(x_0, 0)$  to  $(x_\tau, \tau)$ . Consistently with the adopted notation we write  $R_{\bullet|0,\tau}$  for its law.

#### 3.2 Reciprocal Processes

Jamison (1974) studies the properties of reciprocal processes. A process  $X$  on  $[0, \tau]$  is reciprocal if  $\forall s, t : 0 \leq s < t \leq \tau$ ,

$$\Pr[A_{(s,t)^c} \cap B_{(s,t)} | X_s, X_t] = \Pr[A_{(s,t)^c} | X_s, X_t] \Pr[B_{(s,t)} | X_s, X_t],$$

whenever  $A_{(s,t)^c}$  belongs to the  $\sigma$ -algebra generated by  $\{X_r : 0 \leq r < s\}$  or  $\{X_r : t < r \leq \tau\}$  and  $B_{(s,t)}$  to the  $\sigma$ -algebra generated by  $\{X_r : s < r < t\}$ . A Markov processes is reciprocal, but the converse does not hold without further conditions. In Jamison (1974) it is shown that tying down a Markov process at its initial and terminal values and taking a mixture over such values yields a reciprocal processes. For a process obtained through this construction,

<sup>1</sup>It is a particular case of (18), obtained by Doob h-transform, for  $\Gamma = \delta_{x_0}$  and  $\Upsilon = \delta_{x_\tau}$ .

Jamison (1974, Theorem 3.1) characterizes the cases in which the resulting process is not only reciprocal but also Markov. Let  $X \sim Q \in \mathcal{P}_C$  be a Markov process, let  $q_{t|s}$  denote the associated family of transition densities, here assumed to exist, be strictly positive and continuous, and let  $C \in \mathcal{P}_2(\Gamma, \Upsilon)$  for some  $\Gamma, \Upsilon \in \mathcal{P}_1$ . Then  $CQ_{\bullet|0,\tau}$  is Markov if and only if  $\exists V_0, V_\tau$   $\sigma$ -finite positive measures over  $\mathbb{R}^d$  such that  $C \ll V_0 \otimes V_\tau$ , for the product measure  $V_0 \otimes V_\tau$ , with density

$$\frac{dC}{dv_0 \otimes v_\tau}(x_0, x_\tau) = q_{\tau|0}(x_\tau|x_0). \quad (17)$$

In particular, if at least one of the marginal distributions of  $C$ , i.e.  $\Gamma, \Upsilon$ , concentrates all mass to a single point, (17) is satisfied and  $CQ_{\bullet|0,\tau}$  is Markov. Moreover, given  $\Gamma, \Upsilon \in \mathcal{P}_1$ , there are unique  $C \in \mathcal{P}_2(\Gamma, \Upsilon)$  and  $V_0, V_\tau$   $\sigma$ -finite positive measures such that (17) holds (Jamison, 1974, Theorem 3.2). Finally,  $C$  of (17) equivalently solves (S<sub>sta</sub>) for  $B = Q_{0,\tau}$ , i.e.  $C = S^*(\Gamma, \Upsilon, Q_{0,\tau}, \mathcal{P}_2)$ . Jamison (1975) specializes these result to the case where  $Q$  is the law of a diffusion process. Thus, let  $Q = R$  where  $R$  is given by the solution to (3). Assuming (17), it is shown that  $CR_{\bullet|0,\tau}$ , and hence the solution to (S<sub>dyn</sub>), is realized by the diffusion

$$\begin{aligned} dX_t &= [\mu_R(X_t, t) + \Sigma_R(X_t, t) \nabla_{X_t} \log h(X_t, t)]dt + \sigma_R(X_t, t)dW_t, \\ h(x, t) &:= \int r_{\tau|t}(x_\tau|x_t)V_\tau(dx_\tau), \\ X_0 &\sim \Gamma, \end{aligned} \quad (18)$$

i.e. by means of Doob h-transform (Rogers and Williams, 2000, Chapter IV.6.39). Typically, (18) is not directly applicable,  $V_\tau$  being analytically unavailable.

### 3.3 Diffusion Mixture Matching

The following results establish that a mixture of diffusion processes can be matched, in terms of marginal distribution, by a single diffusion process. Theorem 1 is established in Brigo (2002, Corollary 1.3) limitedly to finite mixtures and 1-dimensional diffusions. The proof and the required assumptions are deferred to Appendix A.

**Theorem 1** (Diffusion mixture matching). *Consider the family of  $d$ -dimensional SDEs indexed by  $\lambda \in \Lambda$*

$$\begin{aligned} dX_t^\lambda &= \mu^\lambda(X_t^\lambda, t)dt + g^\lambda(X_t^\lambda, t)dW_t^\lambda, \quad t \in [0, \tau], \\ X_0^\lambda &\sim P_0^\lambda, \end{aligned} \quad (19)$$

corresponding to the family of path PMs  $\{P^\lambda\}_{\lambda \in \Lambda}$ . For a mixing PM  $\Psi$  on  $\Lambda$ , let  $\Pi \in \mathcal{P}_C$  be obtained by taking the  $\Psi$ -mixture of (19) over  $\lambda \in \Lambda$ . In particular, define the mixture marginal densities  $\pi_t, t \in (0, \tau)$ , and the mixture initial PM  $\Pi_0$  by

$$\pi_t(x) := \int_\Lambda p_t^\lambda(x)\Psi(d\lambda), \quad \Pi_0(dx) := \int_\Lambda P_0^\lambda(dx)\Psi(d\lambda). \quad (20)$$

Consider the  $d$ -dimensional SDE

$$\begin{aligned} dX_t &= \mu(X_t, t)dt + \sigma(X_t, t)dW_t, \quad t \in [0, \tau], \\ \mu(x, t) &:= \frac{\int_\Lambda \mu^\lambda(x, t)p_t^\lambda(x)\Psi(d\lambda)}{\pi_t(x)}, \\ \sigma(x, t) &:= \frac{\int_\Lambda g^\lambda(x, t)p_t^\lambda(x)\Psi(d\lambda)}{\pi_t(x)}, \\ Y_0 &\sim \Pi_0, \end{aligned} \quad (21)$$

with law  $P$ . Then, under mild conditions, for all  $t \in [0, \tau]$  it holds that  $P_t = \Pi_t$ .

### 3.4 Diffusion Bridge Mixture Transports

In Section 3.1 we introduced diffusion bridges mapping initial values  $x_0$  to terminal values  $x_\tau$ . For  $C \in \mathcal{P}_2(\Gamma, \Upsilon)$ , define the diffusion mixture  $\Pi(C, R_{\bullet|0,\tau}) \in \mathcal{P}_C(\Gamma, \Upsilon)$  as the mixture of diffusion bridges (16) over  $(X_0, X_\tau) \sim C$ , that is  $\Pi(C, R_{\bullet|0,\tau}) := CR_{\bullet|0,\tau}$ . We apply Theorem 1 to the collection of diffusion bridges (16) indexed by their initial and terminal values, i.e.  $\lambda = (x_0, x_\tau)$ ,  $\Lambda = \mathbb{R}^d \times \mathbb{R}^d$ , with mixing distribution  $\Psi(d\lambda) = C(dx_0, dx_\tau)$ . The resulting mixture matching SDE has diffusion coefficient  $\sigma_R(x, t)$  and drift coefficient  $\mu_M(x, t) := \mu_R(x, t) + \Sigma_R(x, t)e(x, t)$  where

$$\begin{aligned} e(x_t, t) &= \frac{\int \nabla_{x_t} \log r_{\tau|t}(x_\tau|x_t) \pi_{t|0,\tau}(x_t|x_0, x_\tau) \Pi_{0,\tau}(dx_0, dx_\tau)}{\int \pi_{t|0,\tau}(x_t|x_0, x_\tau) \Pi_{0,\tau}(dx_0, dx_\tau)} \\ &= \int \nabla_{x_t} \log r_{\tau|t}(x_\tau|x_t) \frac{\pi_{t|0,\tau}(x_t|x_0, x_\tau)}{\pi_t(x_t)} \Pi_{0,\tau}(dx_0, dx_\tau) \\ &= \int \nabla_{x_t} \log r_{\tau|t}(x_\tau|x_t) \Pi_{\tau|t}(dx_\tau|x_t) \\ &= \frac{\mathbb{E}[\nabla_{X_t} \log r_{\tau|t}(X_\tau|X_t)|X_t = x]}{\Pi}. \end{aligned}$$

In conclusion, let  $M(\Pi(C, R_{\bullet|0,\tau})) \in \mathcal{P}_C(\Gamma, \Upsilon)$  be the law of the solution to

$$\begin{aligned} dX_t &= \mu_M(X_t, t)dt + \sigma_R(X_t, t)dW_t, \quad t \in [0, \tau], \\ \mu_M(x, t) &= \mu_R(x, t) + \Sigma_R(x, t) \frac{\mathbb{E}[\nabla_{X_t} \log r_{\tau|t}(X_\tau|X_t)|X_t = x]}{\Pi}, \\ X_0 &\sim \Gamma. \end{aligned} \tag{22}$$

Then  $M(\Pi(C, R_{\bullet|0,\tau}))$  satisfies  $M_t(\Pi(C, R_{\bullet|0,\tau})) = \Pi_t(C, R_{\bullet|0,\tau})$  for all  $t \in [0, \tau]$ . In particular  $M(\Pi(C, R_{\bullet|0,\tau}))$  transports  $\Gamma$  to  $\Upsilon$ . We refer to  $M(\Pi(C, R_{\bullet|0,\tau}))$  as diffusion bridge mixture (DBM) transport based on  $C$ .

Before turning our attention to the iterated application of the DBM transport, we consider two additional related transports. The first transport is simply a specialization of the DBM transport to the case of a degenerate initial distribution,  $\Gamma = \delta_{x_0}$ , resulting in

$$\begin{aligned} dX_t &= \mu_{M,x_0}(X_t, t)dt + \sigma_R(X_t, t)dW_t, \quad t \in [0, \tau], \\ \mu_{M,x_0}(x, t) &= \mu_R(x, t) + \Sigma_R(x, t) \frac{\mathbb{E}[\nabla_{X_t} \log r_{\tau|t}(X_\tau|X_t)|X_t = x, X_0 = x_0]}{\Pi}, \\ X_0 &= x_0. \end{aligned} \tag{23}$$

In view of the results presented in Section 3.2,  $\Pi(\delta_{x_0} \otimes \Upsilon, R_{\bullet|0,\tau})$  is the law of a diffusion process (not only a reciprocal process, as in the general case), specifically  $S^*(\delta_{x_0}, \Upsilon, R, \mathcal{P}_C)$ . Moreover, it is easy to see that Theorem 1 applied to a single diffusion yields that same diffusion, not only a diffusion with matching marginal distributions, i.e.  $M(\Pi(\delta_{x_0} \otimes \Upsilon, R_{\bullet|0,\tau})) = \Pi(\delta_{x_0} \otimes \Upsilon, R_{\bullet|0,\tau})$ . Indeed, it can be verified by direct calculation that (23) and (18) share the same drift coefficient when  $\Gamma = \delta_{x_0}$ . In summary, when  $\Gamma = \delta_{x_0}$ , the DBM transport solves a simple version of ( $S_{\text{dyn}}$ ). This is the setting considered in Wang et al. (2021) to define generative models which do not rely on the reversal approach as in Section 2.5.

The second transport corresponds to constructing the DBM on the reversed time direction. More precisely, the following two approaches equivalently yield the same additional transport:

(i) considering as reference SDE the time reversal of (3) with initial distribution  $\Upsilon$ , constructing the DBM transport based on  $\bar{C} \in \mathcal{P}_2(\Upsilon, \Gamma)$  or; (ii) performing a time reversal of (22). For a given  $C \in \mathcal{P}_2(\Gamma, \Upsilon)$ , we refer to the resulting transport as backward DBM (BDBM) transport based on  $C$ . Its law,  $\bar{M}(\Pi(C, R_{\bullet|0,\tau})) \in \mathcal{P}_{\mathcal{C}}(\Upsilon, \Gamma)$ , is the law of the solution to

$$\begin{aligned} d\bar{X}_t &= v_M(\bar{X}_t, t)dt + \sigma_R(\bar{X}_t, \mathbf{r})dW_t, \quad t \in [0, \tau], \\ v_M(x, t) &= -\mu_R(x, \mathbf{r}) + \nabla \cdot \Sigma_R(x, \mathbf{r}) + \Sigma_R(x, \mathbf{r}) \frac{\mathbb{E}[\nabla_{\bar{X}_t} \log r_{\mathbf{r}|0}(\bar{X}_t | \bar{X}_\tau) | \bar{X}_t = x]}{\Pi}, \\ \bar{X}_0 &\sim \Upsilon. \end{aligned} \quad (24)$$

Then  $\bar{M}(\Pi(C, R_{\bullet|0,\tau}))$  satisfies  $\bar{M}_t(\Pi(C, R_{\bullet|0,\tau})) = \bar{\Pi}_t(C, R_{\bullet|0,\tau})$  for all  $t \in [0, \tau]$ . In particular  $\bar{M}(\Pi(C, R_{\bullet|0,\tau}))$  transports  $\Upsilon$  to  $\Gamma$ . Contrasting (15) with (24) reveals that the only difference between the SGM generative model and the corresponding BDBM transport is the measure with respect to which the expectation in the drift adjustment factor is taken.

We consider the iterated application of the DBM transport, specified in Algorithm 2, where at each step  $i$  the initial-terminal distribution of the DBM transport is used to construct the diffusion bridge mixture for step  $i + 1$ . In Theorem 2 we establish the convergence properties of Algorithm 2. We assume an initial coupling given by the product measure  $\Gamma \otimes \Upsilon$ , as it is trivial to sample from this distribution. The arguments of Theorem 2 do not rely on this choice, and alternatives are briefly considered in Section 5.1. As the BDBM transport is the time reversal of the DBM transport, any step  $i$  of Algorithm 2 can be equivalently formulated on the reverse timescale, resulting in  $\bar{C}^{(i)}$ ,  $\bar{\Pi}^{(i)}$  and  $\bar{M}^{(i)}$ .

---

### Algorithm 2 IDBM

---

**Input:**  $\Gamma, \Upsilon, R_{\bullet|0,\tau}, n$

**Output:**  $\{M^{(i)}\}_{i=0}^n$

- 1:  $C^{(0)} \leftarrow \Gamma \otimes \Upsilon$
  - 2:  $\Pi^{(0)} \leftarrow \Pi(C^{(0)}, R_{\bullet|0,\tau})$
  - 3:  $M^{(0)} \leftarrow M(\Pi^{(0)})$
  - 4: **for**  $i = 1, \dots, n$  **do**
  - 5:  $C^{(i)} \leftarrow M_{0,\tau}^{(i-1)}$
  - 6:  $\Pi^{(i)} \leftarrow \Pi(C^{(i)}, R_{\bullet|0,\tau})$
  - 7:  $M^{(i)} \leftarrow M(\Pi^{(i)})$
  - 8: **end for**
- 

**Theorem 2** (IDBM convergence). *For  $\Gamma, \Upsilon \in \mathcal{P}_1$ ,  $R \in \mathcal{P}_{\mathcal{C}}$  solution to (3) with  $\sigma_R(x, t) = I$ , consider the iterates  $\Pi^{(i)}, M^{(i)} \in \mathcal{P}_{\mathcal{C}}(\Gamma, \Upsilon)$  of Algorithm 2. Assume that<sup>2</sup>: (i)  $D_{KL}(C^{(0)} \parallel S_{0,\tau}^*) < \infty$ ; (ii) for each  $i \geq 0$  the Cameron-Martin-Girsanov theorem hold for  $M^{(i)}$  yielding  $dM^{(i)}/dS^*$  (implying that (22) for  $\Pi = \Pi^{(i)}$  has a unique diffusion solution with law  $M^{(i)}$ , and that  $M^{(i)} \ll S^*$ ). Then: (i)  $\Pi^{(i)} \xrightarrow{\mathcal{L}} S^*$  and  $M^{(i)} \xrightarrow{\mathcal{L}} S^*$  as  $i \rightarrow \infty$ , where  $\xrightarrow{\mathcal{L}}$  denotes converge in law; (ii)  $D_{KL}(\Pi^{(i)} \parallel S^*) \geq D_{KL}(M^{(i)} \parallel S^*) \geq D_{KL}(\Pi^{(i+1)} \parallel S^*)$  for  $i \geq 0$  (implying that  $D_{KL}(M^{(i)} \parallel S^*)$  is non-increasing in  $i$ ); (iii)  $D_{KL}(\Pi(C) \parallel S^*) = D_{KL}(M(C) \parallel S^*)$  if and only if  $\Pi(C) = M(C) = S^*$ .*

---

<sup>2</sup>As in the proof, we denote  $\Pi(C) := \Pi(C, R_{\bullet|0,\tau})$ ,  $M(C) := M(\Pi(C, R_{\bullet|0,\tau}))$ ,  $S^* := S^*(\Gamma, \Upsilon, R, \mathcal{P}_{\mathcal{C}})$ .

It remains to address the problem of inferring the drift terms of (22) or of (24) for each step  $i$  of Algorithm 2. The projection property of conditional expectations once again yields suitable objectives:

$$\begin{aligned}
\mathbb{E}_{\Pi}[\nabla_{X_t} \log r_{\tau|t}(X_{\tau}|X_t)|X_t = x] &= \arg \min_{\alpha(x,t)} \mathbb{L}_{\text{DBM}}(\alpha, \Pi), \\
\mathbb{L}_{\text{DBM}}(\alpha, \Pi) &:= \mathbb{E}_{t \sim \mathcal{U}(0,\tau)} [\varrho_t \mathbb{E}_{\Pi}[\|\alpha(X_t, t) - \nabla_{X_t} \log r_{\tau|t}(X_{\tau}|X_t)\|^2]], \\
\mathbb{E}_{\Pi}[\nabla_{X_t} \log r_{t|0}(X_t|X_0)|X_t = x] &= \arg \min_{\alpha(x,t)} \mathbb{L}_{\text{BDBM}}(\alpha, \Pi), \\
\mathbb{L}_{\text{BDBM}}(\alpha, \Pi) &:= \mathbb{E}_{t \sim \mathcal{U}(0,\tau)} [\lambda_t \mathbb{E}_{\Pi}[\|\alpha(X_t, t) - \nabla_{X_t} \log r_{t|0}(X_t|X_0)\|^2]].
\end{aligned} \tag{25}$$

In (25),  $\varrho_t : (0, \tau) \rightarrow \mathbb{R}_{>0}$  and  $\lambda_t : (0, \tau) \rightarrow \mathbb{R}_{>0}$  are time-dependent regularizers that compensates for the diverging  $\nabla_x \log r_{\tau|t}(y|x)$  as  $t \rightarrow \tau$  and  $\nabla_y \log r_{t|0}(y|x)$  as  $t \rightarrow 0$ .

While we rely exclusively on (25) in the numerical experiments of Section 5, additional inferential objectives can be leveraged. Indeed, under mild conditions, performing inference as described in Section 2.4 on data simulated from  $\Pi$  recovers the drifts  $\mu_M(x, t)$  and  $v_M(x, t)$ . For instance, plugging-in the representation (23) in (11) yields  $\mu_M(x, t) = \arg \max_{\alpha(x,t)} \mathbb{O}_{\text{MLE}}(\alpha, \Pi)$ , while that  $\mu_M(x, t) \approx \arg \min_{\alpha(x,t)} \mathbb{L}_{\text{DM}}(\alpha, \Pi, \Delta t)$  follows directly from the definition of  $\Pi$  by interchanging limits. Proofs are omitted here.

We take a moment to provide several comments on the proposed IDBM procedure, contrasting it with the IPF procedure detailed in Section 2.3:

- (i) the IPF steps generate a sequence of initial-terminal measures  $F_{0,\tau}^{(i)} \in \mathcal{P}_2(\Gamma, \cdot) \cup \mathcal{P}_2(\cdot, \Upsilon)$  that matches one of the target marginal distributions  $\Gamma, \Upsilon$  at a time, thus producing a valid coupling between  $\Gamma$  and  $\Upsilon$  only in the limit where  $(\text{S}_{\text{sta}})$  is solved; in contrast, each IDBM step produces a valid initial-terminal coupling  $C^{(i)} \in \mathcal{P}_2(\Gamma, \Upsilon)$ , with the sequence of coupling being progressively optimal toward solving  $(\text{S}_{\text{sta}})$ ;
- (ii) IPF steps necessarily alternates between forward and backward time directions; each IDBM steps can be solved in either of the time direction (or both);
- (iii) approaches relying on samples from  $F^{(i-1)}$  to solve IPF's step  $i$  suffer from the simulation-inference distribution mismatch  $\bar{F}^{(i-1)} \neq F^{(i)}$  which can negatively impact inferential efficiency; by construction  $\Pi^{(i)}$  and  $M^{(i)}$  share the same marginal distributions, so samples from  $\Pi^{(i)}$  are guaranteed to cover regions of high probability according to  $M^{(i)}$ , thus making inference of the corresponding drift coefficient reliable;
- (iv) the measures resulting from the IPF iterations do not admit a simple marginal-conditional decomposition; in contrast each  $\Pi^{(i)}$  is given by a mixture of Brownian bridges (16).

These points suggest that employing the IDBM can be advantageous in the context of generative models. Point (i) establishes that truncating the IDBM iterations at a finite iteration number does not bias the transport. Even the first iteration of the IDBM procedure produces a valid, even if suboptimal, transport. In Section 5.3 we follow this program as an alternative to the approach detailed in Section 2.5. In contrast, the IPF procedure necessitates to employ many iterations which can be computationally expensive. Nevertheless, when multiple IDBM iterations are desirable, it might prove beneficial to solve the iterations alternating between the forward and backward time directions. As the approximation and discretization errors

cumulate over the iterates, repeatedly solving the IDBM procedure in the same time direction could lead to a terminal distribution progressively deviating from the corresponding target marginal distribution. Points (iii) and (iv) point to potential efficiency gains of the IDBM procedure. Indeed, at step  $i > 1$ , inferring the drift terms of both the IPF and the IDBM requires the numerical discretization and simulation from an SDE associated to step  $i - 1$ . This is computationally expensive: in [Bortoli et al. \(2021\)](#) paths are sampled, cached, and re-used for 100 steps of gradient descent. With this choice, path sampling still amounts to roughly 50% of the total computational time. In the IDBM procedure, simulated paths, which are similarly costly to produce, give raise to samples from  $C^{(i-1)}$ . This time however, each sample from  $C^{(i-1)}$  can in turn be used to generate multiple samples at arbitrary time points from  $\Pi^{(i-1)} = C^{(i-1)}R_{\bullet|0,\tau}$  which, for SDEs usually employed in generative modeling (Section 4), can be done cheaply and exactly (see (30)).

## 4 Reference SDE Class

In this section we introduce a class of reference SDEs. This is achieved in two steps: first we formulate a simple SDE, (26), then we show that SDEs commonly employed in generative models such as [Song et al. \(2021\)](#), (31), are realized through a time change.

Consider the  $d$ -dimensional linear SDE

$$\begin{aligned} dY_t &= -\alpha Y_t dt + \Sigma^{1/2} dW_t, \quad t \geq 0, \\ Y_0 &\sim \Gamma, \end{aligned} \tag{26}$$

yielding  $Y \sim P$ , where  $\alpha \geq 0$  is a scalar and  $\Sigma$  is a positive definite matrix. For  $\alpha = 0$ , (26) is the SDE of a correlated and scaled Brownian motion, otherwise (26) is the SDE of an Ornstein-Uhlenbeck process driven by a correlated and scaled Brownian motion. For  $\alpha = \frac{1}{2}$ , (26) has stationary distribution  $\mathcal{N}_d(0, \Sigma)$ . The transition densities  $p_{t|s}$  of (26) are Gaussian:

$$\begin{aligned} (Y_t | Y_s) &\sim \mathcal{N}_d(Y_s a(s, t), \Sigma v(s, t)), \\ a(s, t) &= e^{-\alpha(t-s)}, \\ v(s, t) &= \begin{cases} t - s, & \text{if } \alpha = 0, \\ \frac{1}{2\alpha}(1 - e^{-2\alpha(t-s)}), & \text{if } \alpha > 0, \end{cases} \end{aligned} \tag{27}$$

and

$$\nabla_{y_s} \log p_{t|s}(y_t | y_s) = \Sigma^{-1} \left( \frac{y_t}{a(s, t)} - y_s \right) \frac{a^2(s, t)}{v(s, t)}, \tag{28}$$

$$\nabla_{y_t} \log p_{t|s}(y_t | y_s) = \Sigma^{-1} \left( y_s a(s, t) - y_t \right) \frac{1}{v(s, t)}, \tag{29}$$

which shows that the diffusion bridge (16) corresponding to (26) remains a linear SDE. From Bayes theorem and the Markov property, for  $0 \leq s < t < u$ ,

$$\begin{aligned} (Y_t | Y_s, Y_u) &\sim \mathcal{N}_d(Y_s \hat{a}(s, t, u) + Y_u \check{a}(s, t, u), \Sigma \tilde{v}(s, t, u)), \\ \hat{a}(s, t, u) &= \frac{v(t, u) a(s, t)}{v(s, t) a^2(t, u) + v(t, u)}, \\ \check{a}(s, t, u) &= \frac{v(s, t) a(t, u)}{v(s, t) a^2(t, u) + v(t, u)}, \\ \tilde{v}(s, t, u) &= \frac{v(s, t) v(t, u)}{v(s, t) a^2(t, u) + v(t, u)}. \end{aligned} \tag{30}$$

Now we consider the following time change of (26). Let  $\beta_t : [0, \tau] \rightarrow \mathbb{R}_{>0}$  be a continuous strictly positive function and  $b_t := \int_0^t \beta_u du$ . Then  $b_t : [0, \tau] \rightarrow [0, b_\tau]$  is differentiable strictly increasing function and  $\beta_t = \frac{db_t}{dt}$ . Consider the time-changed process  $X_t := Y_{b_t}$  on  $[0, \tau]$ . An application of (Øksendal, 2003, Theorem 8.5.1) establishes that  $X_t$  is equivalent in law to the solution to

$$\begin{aligned} dX_t &= -\alpha\beta_t X_t dt + \sqrt{\beta_t} \Sigma^{1/2} dW_t, \quad t \in [0, \tau], \\ X_0 &\sim \Gamma. \end{aligned} \tag{31}$$

That is, SDE (31) corresponds to the evolution of the simpler SDE (26) under a non-linear time wrapping where time flows with instantaneous intensity  $\beta_t$ .

We conclude this section by specializing (15), (22) and (24) to the case of a reference SDE given by (31) with  $\alpha = 0$  and  $\beta_t = 1$ , referring to Appendix B for the more general case. The generative time reversal process (15) is given by

$$\begin{aligned} d\bar{X}_t &= \frac{\mathbb{E}_R[\bar{X}_\tau | \bar{X}_t] - \bar{X}_t}{\tau - t} dt + \Sigma^{1/2} dW_t, \quad t \in [0, \tau], \\ \bar{X}_0 &\sim \Upsilon. \end{aligned}$$

The DBM transport (22) is given by

$$\begin{aligned} dX_t &= \frac{\mathbb{E}_\Pi[X_\tau | X_t] - X_t}{\tau - t} dt + \Sigma^{1/2} dW_t, \quad t \in [0, \tau], \\ X_0 &\sim \Gamma, \end{aligned}$$

while the BDBM transport (24) is given by

$$\begin{aligned} d\bar{X}_t &= \frac{\mathbb{E}_\Pi[\bar{X}_\tau | \bar{X}_t] - \bar{X}_t}{\tau - t} dt + \Sigma^{1/2} dW_t, \quad t \in [0, \tau], \\ \bar{X}_0 &\sim \Upsilon. \end{aligned}$$

In this case the DBM and BDBM transports are symmetric: the DBM transport based on  $C \in \mathcal{P}_2(\Gamma, \Upsilon)$  is equivalent in law to the BDBM transport based on  $\bar{C} \in \mathcal{P}_2(\Upsilon, \Gamma)$ .

## 5 Applications

### 5.1 Gaussian Transports

We investigate in depth the case where both the initial and terminal distributions are  $d$ -dimensional Gaussian distributions,  $\Gamma = \mathcal{N}_d(\mu_0, \Sigma_0)$ ,  $\Upsilon = \mathcal{N}_d(\mu_1, \Sigma_1)$ , and the reference measure  $R$  is associated to  $dX_t = \sigma dW_t$  over the time interval  $[0, 1]$ . The solution to the entropy-regularized OT problem associated to  $(\Gamma, \Upsilon, R)$  is the Gaussian coupling

$$S_{0,1}^*(\Gamma, \Upsilon, R, \mathcal{P}_C) = \mathcal{N}_{2d} \left( \begin{bmatrix} \mu_0 \\ \mu_1 \end{bmatrix}, \begin{bmatrix} \Sigma_0 & \Sigma_S(\sigma) \\ \Sigma_S(\sigma)^\top & \Sigma_1 \end{bmatrix} \right), \tag{32}$$

where  $\Sigma_S(\sigma) := (\Sigma_0 \Sigma_1 + \frac{\sigma^4}{4} I)^{1/2} - \frac{\sigma^2}{2} I$ . The solution  $OT^*(\Gamma, \Upsilon)$  to the OT problem is obtained setting  $\sigma = 0$  in (32)<sup>3</sup>, with corresponding OT plan  $\varphi_{OT}(x) := \mu_1 + \Sigma_0^{-1} \Sigma_S(0)(x - \mu_0)$ . See for instance Peyré and Cuturi (2020, Section 2.6) and Janati et al. (2020, Section 2).

<sup>3</sup>Gaussian distributions with positive semi-definite but not positive definite covariance matrices are well-defined through their characteristic function.

Consider the DBM transport based on the Gaussian coupling  $C \in \mathcal{P}_2(\Gamma, \Upsilon)$

$$C = \mathcal{N}_{2d} \left( \begin{bmatrix} \mu_0 \\ \mu_1 \end{bmatrix}, \begin{bmatrix} \Sigma_0 & \Sigma_C \\ \Sigma_C^\top & \Sigma_1 \end{bmatrix} \right). \quad (33)$$

The mixture of diffusion bridges with law  $\Pi(C, R_{\bullet|0,1})$  has a joint distribution  $\Pi_{0,t,1}(C, R_{\bullet|0,1})$  which is again Gaussian

$$\Pi_{0,t,1}(C, R_{\bullet|0,1}) = \mathcal{N}_{3d} \left( \begin{bmatrix} \mu_0 \\ (1-t)\mu_0 + t\mu_1 \\ \mu_1 \end{bmatrix}, \begin{bmatrix} \Sigma_0 & \Sigma_{\Pi;0,t} & \Sigma_C \\ \Sigma_{\Pi;0,t}^\top & \Sigma_{\Pi;t,t} & \Sigma_{\Pi;t,1} \\ \Sigma_C^\top & \Sigma_{\Pi;t,1}^\top & \Sigma_1 \end{bmatrix} \right),$$

where  $\Sigma_{\Pi;0,t} = (1-t)\Sigma_0 + t\Sigma_C$ ,  $\Sigma_{\Pi;t,t} = (1-t)^2\Sigma_0 + t^2\Sigma_1 + t(1-t)(\Sigma_C + \Sigma_C^\top + \sigma^2 I)$  and  $\Sigma_{\Pi;t,1} = (1-t)\Sigma_C + t\Sigma_1$ . It follows that

$$\mathbb{E}_{\Pi}[X_1|X_t] = \mu_1 + \Sigma_{\Pi;t,1}^\top \Sigma_{\Pi;t,t}^{-1} (X_t - \mu_t)$$

and the DBM transport with law  $M(\Pi(C, R_{\bullet|0,1}))$  is given by the solution to

$$dX_t = \frac{\mathbb{E}_{\Pi}[X_1|X_t] - X_t}{1-t} dt + \sigma dW_t, \quad t \in [0, 1], \quad (34)$$

$$X_0 \sim \Gamma.$$

SDE (34) is of the form  $dX_t = (A_t X_t + b_t) dt + \sigma dW_t$  for  $A_t : [0, 1] \rightarrow \mathbb{R}^{d \times d}$ ,  $b_t : [0, 1] \rightarrow \mathbb{R}^d$ , i.e. it is linear and time-inhomogenous with Gaussian transition probabilities. The following representation holds:  $X_1|X_0$  is distributed as  $P_1 X_0 + \varepsilon$ , where  $P_t$  is given by the solution to the matrix-valued ODE

$$dP_t = A_t P_t, \quad t \in [0, 1], \quad (35)$$

$$P_0 = I,$$

and  $\varepsilon$  is a  $d$ -dimensional Gaussian distribution whose parameters depend on the functions  $A_t$  and  $b_t$ , but not on  $X_0$ . In conclusion,

$$M_{0,t}(\Pi(C, R_{\bullet|0,1})) = \mathcal{N}_{2d} \left( \begin{bmatrix} \mu_0 \\ \mu_1 \end{bmatrix}, \begin{bmatrix} \Sigma_0 & \Sigma_{C'} \\ \Sigma_{C'}^\top & \Sigma_1 \end{bmatrix} \right), \quad \Sigma_{C'} := \Sigma_0 P_1^\top. \quad (36)$$

Starting from the Gaussian coupling  $C^{(0)} = \Gamma \otimes \Upsilon$ , i.e.  $\Sigma_{C^{(0)}} = 0I$ , the IDBM procedure iteratively computes the updates  $\Sigma_C \rightarrow \Sigma_{C'}$  resulting in sequence of Gaussian couplings  $C^{(i)}$ .

The IPF updates for  $(S_{\text{sta}})$  can be computed analytically thanks to the following property of Gaussian distributions. Let  $X$  and  $Y$  be  $d$ -dimensional random variables with  $(X, Y) \sim P_{X,Y}$ , where

$$P_{X,Y} := \mathcal{N}_{2d} \left( \begin{bmatrix} \mu_x \\ \mu_y \end{bmatrix}, \begin{bmatrix} \Sigma_{xx} & \Sigma_{xy} \\ \Sigma_{xy}^\top & \Sigma_{yy} \end{bmatrix} \right),$$

and denote with  $P_{Y|X}$  the conditional distribution of  $Y$  given  $X$  under  $P_{X,Y}$ . For  $Q_X := \mathcal{N}_d(\lambda_x, \Gamma_{xx})$ , we have

$$Q_X P_{Y|X} = \mathcal{N}_{2d} \left( \begin{bmatrix} \lambda_x \\ \lambda_y \end{bmatrix}, \begin{bmatrix} \Gamma_{xx} & \Gamma_{xy} \\ \Gamma_{xy}^\top & \Gamma_{yy} \end{bmatrix} \right), \quad (37)$$

$$\lambda_y := \mu_y + \Sigma_{xy}^\top \Sigma_{xx}^{-1} (\lambda_x - \mu_x),$$

$$\Gamma_{xy} := \Gamma_{xx} \Sigma_{xx}^{-1} \Sigma_{xy},$$

$$\Gamma_{yy} := \Sigma_{yy} + \Sigma_{xy}^\top (\Sigma_{xx}^{-1} \Gamma_{xx} \Sigma_{xx}^{-1} - \Sigma_{xx}^{-1}) \Sigma_{xy}.$$

Therefore, starting from

$$F_{0,1}^{(0)} = \mathcal{N}_{2d} \left( \begin{bmatrix} \mu_0 \\ \mu_0 \end{bmatrix}, \begin{bmatrix} \Sigma_0 & \Sigma_0 \\ \Sigma_0 & \Sigma_0 + \sigma^2 I \end{bmatrix} \right),$$

the IPF iterations update one of the marginal distributions of  $F_{0,1}^{(i)}$  at a time via (37).

When  $d = 1$ , ODE (35) can be solved analytically. The coupling distribution (33) has a single degree of freedom, its correlation coefficient, which we denote with  $\rho_C$ . Then,  $M_{0,1}(\Pi(C, R_{\bullet|0,1})) \in \mathcal{P}_2(\Gamma, \Upsilon)$  is Gaussian with correlation coefficient

$$\begin{aligned} \rho_M(\rho_C, \Sigma_0, \Sigma_1, \sigma) &:= \exp \left\{ -\sigma^2 \frac{\tanh^{-1}(\frac{c_1}{c_3}) + \tanh^{-1}(\frac{c_2}{c_3})}{c_3} \right\} \\ c_1 &= \sigma^2 + 2\Sigma_1(\rho_C \Sigma_0 - \Sigma_1), c_3 = \sqrt{(\sigma^2 + 2(\rho_C + 1)\Sigma_0 \Sigma_1)(\sigma^2 + 2(\rho_C - 1)\Sigma_0 \Sigma_1)}, \\ c_2 &= \sigma^2 + 2\Sigma_0(\rho_C \Sigma_1 - \Sigma_0), \end{aligned} \quad (38)$$

which is independent of  $\mu_0, \mu_1$ . The following results hold: (i) for fixed  $\sigma, \Sigma_0, \Sigma_1$ , the map  $\rho_M(\rho, \Sigma_0, \Sigma_1, \sigma) : \rho \mapsto \rho'$  is a contraction over  $\rho \in [-1, 1]$  with limiting value  $(\sqrt{\Sigma_0 \Sigma_1 + \frac{\sigma^4}{4}} - \frac{\sigma^2}{2}) / \sqrt{\Sigma_0 \Sigma_1}$ , i.e. the correlation coefficient of the solution to the entropy-regularized OT problem; (ii) for fixed  $\rho, \Sigma_0, \Sigma_1$ ,  $\lim_{\sigma \rightarrow 0} \rho_M(\rho, \Sigma_0, \Sigma_1, \sigma) = \rho_M(\rho, \Sigma_0, \Sigma_1, 0) = 1$ , i.e. the correlation coefficient of  $OT^*(\Gamma, \Upsilon)$ . Result (i) establishes that the couplings produced by the IDBM iterations converge to  $S_{0,1}^*(\Gamma, \Upsilon, R, \mathcal{P}_C)$ , as expected from Theorem 2. Result (ii) shows that the DBM transport remains well-posed for vanishing regularization  $\sigma$ , and that  $\Pi_{0,1}^{(1)} \xrightarrow{\mathcal{L}} OT^*(\Gamma, \Upsilon)$  as  $\sigma \rightarrow 0$ , i.e. convergence (in law) is attained by the first iteration of the IDBM procedure. To gain more insight, consider once again the DBM SDE  $dX_t = (A_t X_t + b_t)dt + \sigma dW_t$ . In the noiseless limit  $\sigma \rightarrow 0$ , the dynamics are specified by the DBM ODE  $dx_t = (A_t^0 x_t + b_t^0)dt$ , where  $A_t^0 := \lim_{\sigma \rightarrow 0} A_t$  and  $b_t^0 := \lim_{\sigma \rightarrow 0} b_t$ . Moreover, the solution  $M$  to the DBM SDE converges in probability to the solution to the DBM ODE (Stroock and Varadhan, 2006, Chapter 11). Solving the DBM ODE and computing the solution at terminal time yields  $x_1 = \mu_1 + \sqrt{\Sigma_1 / \Sigma_0}(x_0 - \mu_0) = \varphi_{OT}(x_0)$ , the OT plan.

We consider the scenario  $\mu_0 = -1, \mu_1 = 1, \Sigma_0 = \Sigma_1 = \sigma^2 = 1$ . We compute the KL divergence from the IPF PMs  $F_{0,1}^{(i)}$  and the IDBM couplings  $\Pi_{0,1}^{(i)}$  to the solution  $S_{0,1}^*(\Gamma, \Upsilon, R, \mathcal{P}_C)$  to  $(S_{\text{sta}})$  as function of the iterations. The KL divergence between multivariate Gaussian distributions is available analytically, so no approximation is required. The results are shown in Figure 1 where, in addition to the standard initial independent coupling  $C^{(0)} = \Gamma \otimes \Upsilon$ , we consider two additional initial couplings with correlations  $\rho_{C^{(0)}} = \pm 1$ . It is observed that the IDBM iterations exhibit a faster rate of convergence with respect to the KL divergence. We remark that with our choice of indexing for the IPF procedure we are slightly favoring the IPF iterations, in the sense that  $F_{0,1}^{(0)}$  already incorporates the reference measure  $R$ , while  $C^{(0)}$  does not depend on  $R$ . In Figure 2 we modify the considered scenario by varying the level of regularization:  $\sigma = 10^s$  for  $s = -2, \dots, 2$ , with  $\sigma = 10^{-2}$  corresponding to the blue color and  $\sigma = 10^2$  to the red color. While the IDBM iterations converge quickly for both low and high levels of regularization (with  $\sigma = 1$ , as in Figure 1, exhibiting the slowest convergence), the IPF iterations display increasing KL divergence for vanishing  $\sigma$ .

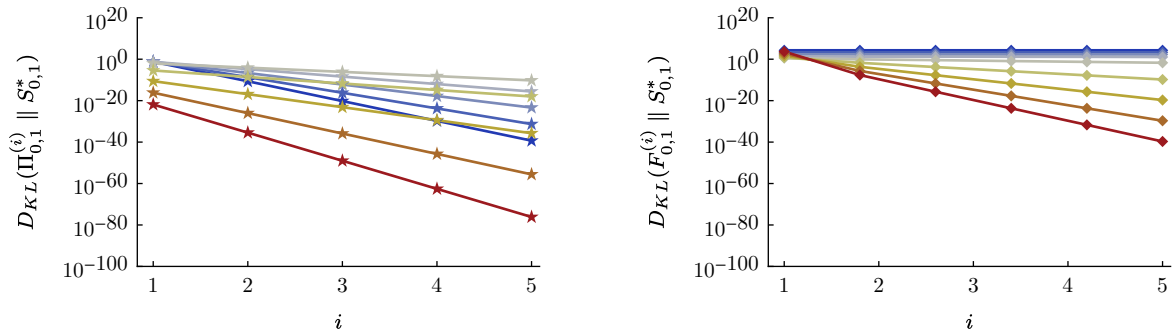


Figure 2: Same as Figure 1 for varying levels of regularization  $\sigma$ ; (left): IDBM; (right): IPF;  $d = 1$ ; shared log-scale.

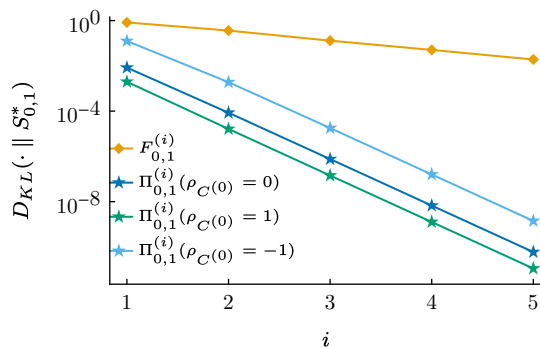


Figure 1: Convergence of IPF and IDBM initial-terminal PMs to  $S_{0,1}^*$  in KL divergence;  $d = 1$ ; log-scale.

lim	$D_{KL}(\Pi_{0,1}^{(1)} \  S_{0,1}^*)^4$	$D_{KL}(F_{0,1}^{(1)} \  S_{0,1}^*)$
$\mu_{\{0,1\}} \rightarrow \pm\infty$	$k$	$\infty$
$\Sigma_{\{0,1\}} \rightarrow \infty$	$K_{\Pi}$	$\infty$
$\Sigma_{\{0,1\}} \rightarrow 0$	$0$	$k$
$\sigma \rightarrow \infty$	$0$	$0$
$\sigma \rightarrow 0$	$k$	$\infty$

Table 1: Summary of limiting behavior of the first iteration of the IDBM and IPF procedures.

We complete the analysis of the one-dimensional setting by studying the behavior of  $D_{KL}(\Pi_{0,1}^{(1)} \| S_{0,1}^*)$  and  $D_{KL}(F_{0,1}^{(1)} \| S_{0,1}^*)$  at the boundaries of the parameters' space spanned by  $\theta = (\mu_0, \mu_1, \Sigma_0, \Sigma_1, \sigma)$ . The results are shown in Table 1, where  $k$  denotes positive finite values,  $K_{\Pi} := \frac{1}{4}(\pi + \log[4] - 2(1 + \log[\pi]))$  is the supremum of  $D_{KL}(\Pi_{0,1}^{(1)} \| S_{0,1}^*)$  over  $\theta$ ,  $\mu_{\{0,1\}}$  stands for either of  $\mu_0, \mu_1$ , and  $\Sigma_{\{0,1\}}$  stands for either of  $\Sigma_0, \Sigma_1$ . When taking each limit all other parameters are kept constant. Note that all of  $\Pi_{0,1}^{(1)}, F_{0,1}^{(1)}$  and  $S_{0,1}^*$  depend on  $\theta$ , even though the notation does not make this explicit. The results of Table 1 support the robustness of the IDBM procedure in the one-dimensional setting.

For  $d > 1$ , we numerically integrate the matrix-valued ODE (35). We generate 20 scenarios for each of  $d = 5, 10$ . In each scenario, we sample  $\mu_0, \mu_1$  uniformly on  $[-1, 1]^d$  and  $\Sigma_0, \Sigma_1$  from a Wishart distribution with  $d$  degrees of freedom and covariance matrix  $0.2I$  (as in Janati et al. (2020)). We set  $\sigma = 0.2$  when  $d = 5$  and  $\sigma = 1$  when  $d = 10$ . In the multivariate instance,  $\Pi_{0,1}^{(1)}$  does not converge to  $OT^*(\Gamma, \Upsilon)$  as  $\sigma \rightarrow 0$ , and the convergence rate the IDBM procedure worsens as  $\sigma$  approaches 0. Indeed, in the Gaussian setting defined for this study, the  $\sigma \rightarrow 0$  limit of the DBM transport is equivalent to the rectified flow of Liu et al. (2022), and the authors of Liu (2022) show that the rectified flow solves the OT problem only in the one-dimensional case. Nonetheless, the IDBM procedure continues to outperform the IPF

<sup>4</sup> $D_{KL}(\Pi_{0,1}^{(1)} \| S_{0,1}^*)$  is independent of  $\mu_{\{0,1\}}$ .

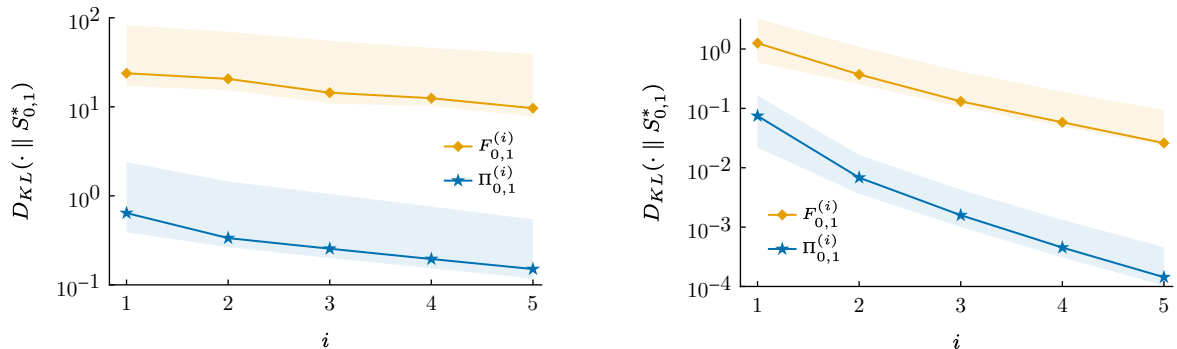


Figure 3: Convergence of IPF and IDBM initial-terminal PMs to  $S_{0,1}^*$  in KL divergence; (left):  $d = 5$ ; (right):  $d = 10$ ; log-scale.

procedure in the considered scenarios. In Figure 3 we plot the average KL divergences from  $\Pi_{0,1}^{(1)}$  and  $F_{0,1}^{(1)}$  to  $S_{0,1}^*$  as function of the iterations with solid lines, where each average is over 20 scenarios. The banded regions correspond to the ranges between the worsts and the bests KL divergence values across the scenarios.

## 5.2 Mixture Transports

We consider  $\Gamma := \frac{1}{3}(\mathcal{N}_1(-3, 0.2^2) + \mathcal{N}_1(0.5, 0.2^2) + \mathcal{N}_1(3, 0.2^2))$ ,  $\Upsilon := \mathcal{N}_1(0, 2^2)$  and  $R$  associated to  $dX_t = \sigma dW_t$  over the time interval  $[0, 1]$ , for  $\sigma = 0.2$ . This configuration is selected to illustrate the limitation of the sample-based diffusion IPF procedures discussed in Section 2.3.

Our goal is to construct a transport from  $\Upsilon$  to  $\Gamma$ . This toy experiment can be seen as a simplified instance of the generative setting introduced in Section 2.5: the training data consists of the values  $\{-3, 0.5, 3\}$  and  $\Gamma = D_\eta$  for  $\eta = 0.2$ . Compared with typical applications,  $\sigma$  has been set to a small value to introduce a strong dependency between  $X_0$  and  $X_1$  under  $R$ , making SGM approaches inapplicable.

For the remainder of this Section, we always assume that time  $t$  flows in the generative direction  $\Upsilon \rightarrow \Gamma$ . The first iteration of the IPF procedure relies on samples from  $R$  to infer  $\mu_{F^{(1)}}(x, t)$ . We display  $\mu_{F^{(1)}}(x, t)$  in Figure 4 (bottom-left), superimposing with gray lines the level sets of the marginal densities  $r_t$ ,  $t \in [0, 1]$ . It can be seen that samples from  $R$  have negligible probability of falling outside narrowly defined regions. We consider a fully-connected neural network  $\alpha_\theta(x, t)$  with 3 hidden layers, the ReLU ( $x \rightarrow \max(0, x)$ ) activation function, and a width of 512 units. Using objective (13),  $\alpha_\theta(x, t)$  is optimized via stochastic gradient descent (SGD). We display the resulting inferred drift function at convergence  $\alpha_{F^{(1)}}(x, t)$  in Figure 4 (bottom-center), again superimposing the level sets of  $r_t$ . The approximation is very good in regions of high probability under  $R$ , but significant deviations can be observed outside these regions. We contrast the true density of  $F_1^{(1)}$  with a kernel density estimate based on 10 million samples from  $\widehat{F}_1^{(1)}$ , which are obtained by applying the Euler scheme,  $\Delta t = 10^{-4}$ , to

$$\begin{aligned} dX_t &= \alpha_{F^{(1)}}(X_t, t)dt + \sigma dW_t, \quad t \in [0, 1], \\ X_0 &\sim \Upsilon, \end{aligned}$$

and collecting the terminal states. As show in Figure 4 (bottom-right), the approximation errors have a significant impact. Implementing sample-based diffusion IPF procedures for generative purposes requires carefully choosing the level of regularization. On one hand, a too

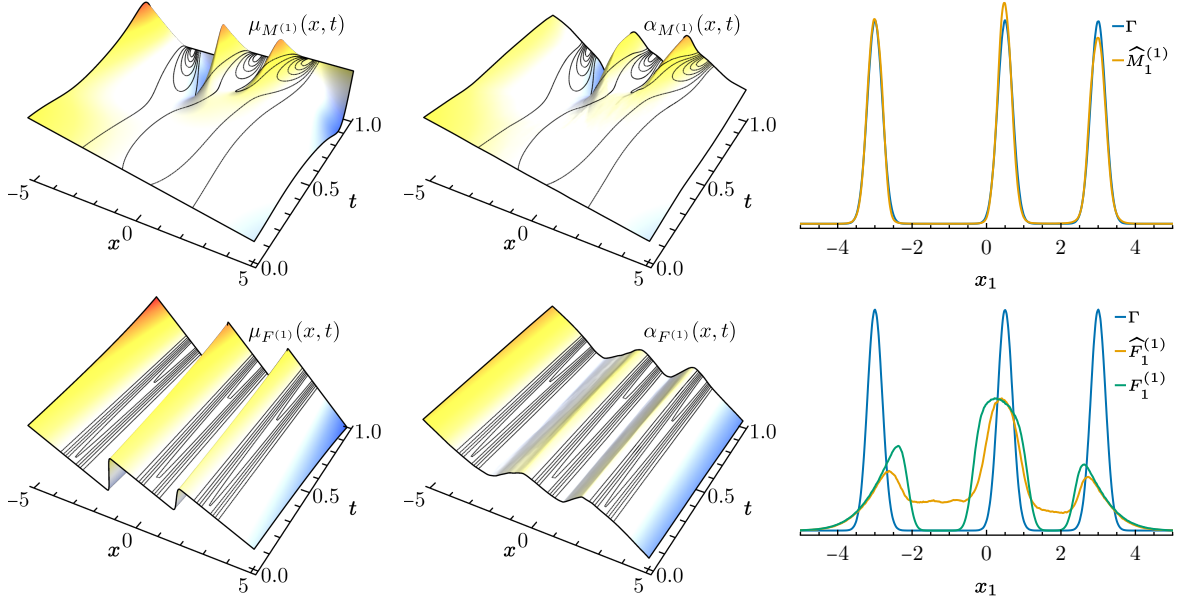


Figure 4: Drift (left), estimated drift (center) and terminal density (right) resulting from the first iteration of the IPF (bottom) and IDBM (top) procedures; generative time.

high level of  $\sigma$  renders IPF iterations after the first superfluous, as  $F^{(1)}$  approximately solves  $(S_{\text{dyn}})$ . On the other hand, a too low level of  $\sigma$  risks incurring in the difficulties just exposed.

We construct the IDBM transport based on  $\Upsilon \otimes \Gamma$ . The drift  $\mu_{M^{(1)}}(x, t)$  corresponding to the first IDBM iteration is shown in Figure 4 (top-left), superimposed with gray lines representing the level sets of the marginal densities  $\pi_t^{(1)}$ ,  $t \in [0, 1]$ . Drift inference is based on samples from  $\Pi^{(1)}$ . The same neural network architecture is employed, and using objective (25)  $\alpha_\theta(x, t)$  is optimized via SGD. We display the resulting inferred drift function at convergence  $\alpha_{M^{(1)}}(x, t)$  in Figure 4 (top-center) superimposing the level sets of  $\pi_t^{(1)}$ . As expected,  $\alpha_{M^{(1)}}(x, t)$  closely approximates  $\mu_{M^{(1)}}(x, t)$  in regions of high probability under  $\Pi^{(1)}$ . Crucially, this suffices for learning  $\mu_{M^{(1)}}(x, t)$  on the regions of the path space relevant for the simulation from  $M^{(1)}$ . We contrast the true density of  $\Gamma$  with a kernel density estimate based on 10 million samples from  $\widehat{M}_1^{(1)}$ , which are obtained by applying the Euler scheme,  $\Delta t = 10^{-4}$ , to

$$\begin{aligned} dX_t &= \alpha_{M^{(1)}}(X_t, t)dt + \sigma dW_t, \quad t \in [0, 1], \\ X_0 &\sim \Upsilon, \end{aligned}$$

and collecting the terminal states. The close agreement between  $\Gamma$  and  $\widehat{M}_1^{(1)}$  is shown in Figure 4 (top-right).

We discretize  $\Upsilon$  and  $\Gamma$  into 5000 equally spaced bins on  $[-5, 5]$  and solve the corresponding entropy-regularized problem using the Sinkhorn algorithm from the POT library (Flamary et al., 2021). For  $\sigma = 0.2$ , convergence is attained in around 2000 iterations with default tolerances. We display the resulting 2D histogram in Figure 5 (left). We additionally show the 2D kernel density estimates based on the samples from  $\widehat{F}^{(1)}$  (center) and  $\widehat{M}^{(1)}$  (right). It can be seen that the first iteration of the IDBM procedure suffices to produce a coupling capturing the overall shape of  $S_{0,1}^*$ .

We conclude this section with two remarks. In the setting of this experiment, the drift

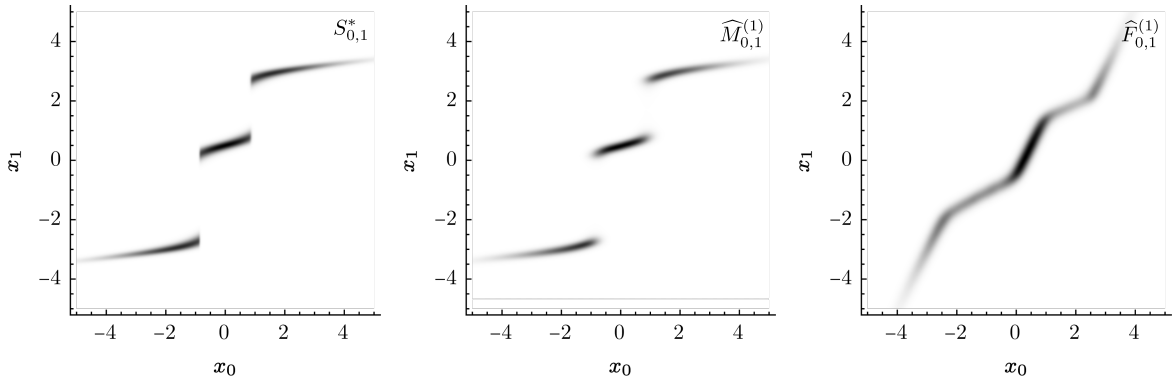


Figure 5: Optimal coupling (left), coupling from the first iteration of the IDBM procedure (center), PM from the first iteration of the IPF procedure (right); generative time.

coefficient  $\mu_{M^{(1)}}(x, t)$  is smoother<sup>5</sup> than  $\mu_{F^{(1)}}(x, t)$ . This aspect makes it easier both to approximate  $\mu_{M^{(1)}}(x, t)$  with a neural network and to accurately simulate from the resulting SDE. In the case of the Gaussian transports of Section 5.1, for each  $i$  and  $t$ ,  $F_t^{(i)}$  is a multivariate Gaussian distribution (Mallasto et al., 2022). Therefore,  $\mu_{F^{(i)}}(x, t)$  is an affine function in  $x$  for every  $i$  and  $t$ , in which case local information about  $\mu_{F^{(i)}}(x, t)$  is global as well, and the simulation-inference discrepancy has no impact on the efficiency of the inference procedure.

### 5.3 Generative Modeling

In this section we explore the use of the BDBM transport, as an alternative to the score-based generative paradigm of Section 2.5, for image generation purposes. The reference SDE is given by (31) with  $\alpha = 0$  and  $\Sigma = I$ , i.e. by a scaled  $d$ -dimensional Brownian motion. We consider the CIFAR-10 dataset, hence  $d = 28 \times 28 \times 3$ . As baseline modeling choice we consider the “VE SDE” parametrization from Song et al. (2021) for  $\beta_t$ , and the corresponding smoothed training data distribution  $D_\eta$ :

$$\begin{aligned}
 dX_t &= \sqrt{\beta_t} dW_t, \quad t \in [0, 1], \\
 X_0 &\sim D_\eta, \\
 \beta_t &:= \sigma_{\min}^2 \left( \frac{\sigma_{\max}}{\sigma_{\min}} \right)^{2t} 2 \log \left( \frac{\sigma_{\max}}{\sigma_{\min}} \right), \\
 b_t &= \sigma_{\min}^2 \left( \frac{\sigma_{\max}}{\sigma_{\min}} \right)^{2t} - \sigma_{\min}^2,
 \end{aligned} \tag{39}$$

where  $\eta = \sigma_{\min} = 10^{-2}$  and  $\sigma_{\max} = 50$ . We recall that  $D_\eta := \frac{1}{n} \sum_{s=1}^n \mathcal{N}_d(x_s; 0, \eta^2 I_d)$ . Here  $x_1, \dots, x_n$  are the  $n = 50,000$  samples of CIFAR-10’s training dataset  $D_{\text{CIFAR-10}}^{\text{train}}$ . We select the NCSN++ (smaller) architecture, and training is performed using the official PyTorch implementation<sup>6</sup> of Song et al. (2021). We review the SGM training procedure in Algorithm 3.

<sup>5</sup>Both drift coefficients are analytical functions.

<sup>6</sup>[https://github.com/yang-song/score\\_sde\\_pytorch](https://github.com/yang-song/score_sde_pytorch).

---

**Algorithm 3** SGM training

---

**Input:**  $\Gamma, R_{t|0}, \nabla_y \log r_{t|0}(y, x), \alpha_\theta(x, t)$ **Output:**  $\alpha_{\text{SGM}}(x, t)$ 

- 1: **repeat**
  - 2:  $t \sim \mathcal{U}(0, \tau)$
  - 3:  $X_0 \sim \Gamma$
  - 4:
  - 5:  $X_t \sim R_{t|0}(\cdot | X_0)$
  - 6:  $Y_t \leftarrow \nabla_{X_t} \log r_{t|0}(X_t | X_0)$
  - 7:  $\mathcal{L} \leftarrow \|Y_t - \alpha_\theta(X_t, t)\|^2 \lambda_t$
  - 8:  $\theta \leftarrow \text{sgdstep}(\theta, \mathcal{L})$
  - 9: **until** convergence
- 

---

**Algorithm 4** BDBM training

---

**Input:**  $\Gamma, \Upsilon, R_{t|0, \tau}, \nabla_y \log r_{t|0}(y, x), \alpha_\theta(x, t)$ **Output:**  $\alpha_{\text{BDBM}}(x, t)$ 

- 1: **repeat**
  - 2:  $t \sim \mathcal{U}(0, \tau)$
  - 3:  $X_0 \sim \Gamma$
  - 4:  $X_\tau \sim \Upsilon$
  - 5:  $X_t \sim R_{t|0, \tau}(\cdot | X_0, X_\tau)$
  - 6:  $Y_t \leftarrow \nabla_{X_t} \log r_{t|0}(X_t | X_0)$
  - 7:  $\mathcal{L} \leftarrow \|Y_t - \alpha_\theta(X_t, t)\|^2 \lambda_t$
  - 8:  $\theta \leftarrow \text{sgdstep}(\theta, \mathcal{L})$
  - 9: **until** convergence
- 

Implementing the BDBM approach requires minimal changes, as delineated in Algorithm 4. PyTorch implementations of SGM and BDBM losses are provided for a reference SDE described by (31) with  $\Sigma = I$  and for the regularizer  $\lambda_t = v(0, t)$  in Listings 1 and 2 of Appendix C.

By design, the reference process in (39) strongly decouples  $X_1$  from  $X_0$ , in which case the BDBM and SGM approaches yield similar generative models. We set  $\sigma_{\max} = 1$  and keep  $\Upsilon = \mathcal{N}_d(0, \sigma_{\max}^2 I)$  for the generative process’s initial distribution, without making efforts to optimize these hyperparameters. Apart from the aforementioned modifications to the loss function, no additional changes are introduced to the training code, and training proceeds as for the baseline SGM.

The trained neural network approximators obtained from Algorithm 3 and Algorithm 4 corresponds to the drift multiplicative factors appearing in (15) and (24) as conditional expectations. As the remaining terms in (15) and (24) are identical, no code changes are necessary when transitioning from SGM to BDBM at generation time.

In order to assess the visual quality of generated samples, the Fréchet Inception Distance (FID, Heusel et al. (2017)) is employed. FID, which aligns with human-perceived visual quality, is calculated as the 2-Wasserstein Euclidean distance in features space, where image features are derived from the Inception model architecture. CIFAR-10 training occurs over 1.300.000 SGD steps. Every 50.000 steps, the FIDs between the test portion of the CIFAR-10 dataset,  $D_{\text{CIFAR-10}}^{\text{test}}$ , and corresponding 5.000 samples generated from the SGM and BDBM models are computed. Sampling is performed using the Euler scheme (10),  $\Delta t = 10^{-3}$ . The results are presented in Figure 6, illustrating the competitive performance of the BDBM model for this discretization interval. Furthermore, the BDBM approach exhibits significantly faster training.

For each of the considered models and their 26 parameter states (checkpoints), generating 5.000 samples from either the SGM or the BDBM model using the Euler scheme with a discretization interval  $\Delta t = 10^{-4}$  necessitates approximately one day of computation on the NVIDIA RTX 3090 GPU utilized in this experiment. With the same discretization interval, the predictor-corrector scheme of Song et al. (2021) demands twice the computation time. Consequently, our analysis is restricted to the Euler scheme and a single “optimal” checkpoint is selected for both the SGM and BDBM models based on the findings of Figure 6. For the BDBM model, we opt for the model trained for 250.000 steps, while for the SGM

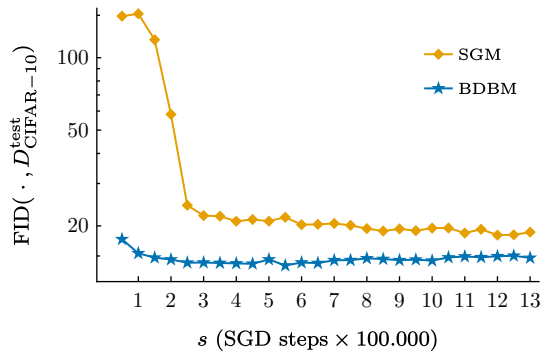


Figure 6: FID between samples generated from the SGM and BDBM models and CIFAR-10 test empirical distribution at  $\Delta t = 10^{-3}$ ; log-scale.



Figure 7: Samples from the SGM and BDBM models with different discretization intervals, compared to samples from the CIFAR-10 training dataset.

model we select the model trained for 1.200.000 steps, which aligns with the checkpoint chosen in Song et al. (2021). Subsequently, we calculate the FID values corresponding to  $\Delta t = 1/25, 1/100, 1/1000$ , obtaining 93.7, 14.0, 12.1 for the BDBM model and 420.3, 18.3, 12.0 for the SGM model, respectively. Corresponding randomly selected samples are shown in Figure 7 and contrasted with the first 16 CIFAR-10 training samples. Although the visual quality of the SGM and BDBM models is comparable at finer discretization steps, the BDBM model retains superior visual quality as the discretization interval increases.

## 6 Discussion

In this paper we introduced a novel iterative algorithm, the IDBM transport, aimed at solving the dynamic Schrödinger bridge problem ( $S_{\text{dyn}}$ ), and performed a preliminary theoretical analysis of its convergence properties. The theoretical findings were complemented by various numerical simulations and analytical results, demonstrating the competitive performance of

the IDBM procedure in comparison to the IPF procedure.

As in Pavon et al. (2018); Bortoli et al. (2021); Vargas et al. (2021), we assume that samples from the initial and terminal distributions are either readily available, belonging to some dataset of interest, or can be generated without further approximations. The IDBM transport is particularly suitable for scenarios where the reference diffusion measure  $R$  admits simple analytical transition probabilities. These considerations suggest that the IDBM procedure is ideally suited for current generative applications. Since the IDBM procedure produces a valid coupling at each iteration, we utilize the first IDBM iteration, i.e. the (backward) DBM transport, as an alternative to the approach of Song et al. (2021). This alternative achieves faster training convergence and superior sample quality at broader discretization intervals. An additional advantage of this proposal is the simplicity of its implementation, which differs from the approach of Song et al. (2021) only in the loss definition.

The time-reversal sample-based implementations of Bortoli et al. (2021); Vargas et al. (2021) suffer from the simulation-inference mismatch demonstrated in the present work, and might be difficult to scale to demanding generative applications due to the ensuing lower efficiency and higher computational cost. Building on a previous version of the current paper, Wu et al. (2022); Liu et al. (2023) successfully employ the DBM transport in a wide range of applications. Furthermore, in Liu et al. (2023) the DBM transport is shown to correspond to an optimal Markovianization of the mixture of diffusion bridges whose marginal distributions it matches. Concurrently and independently of our research, Shi et al. (2023) introduces the *Diffusion Schrödinger Bridge Matching (DSBM)* procedure, which is equivalent to the IDBM procedure discussed in the current paper. Shi et al. (2023) conducts a preliminary theoretical assessment of the convergence properties of the *DSBM* procedure and empirically compares it with the proposal of Bortoli et al. (2021). One of the numerical experiments pertains to the Gaussian setting detailed in Section 5.1, with  $\Sigma_0 = \Sigma_1 = I$  and  $d = 50$ . In contrast to our investigation, neural networks approximators are utilized and trained iteratively. The subsequent results are consistent with our findings of Section 5.1, illustrating the competitive performance of the *DSBM* procedure. Lastly, Shi et al. (2023) performs an extensive survey of a vast and expanding corpus of recent literature which focuses on the development of deterministic and stochastic transports for generative modeling applications. Numerous transports within this body of work are shown to bear a close relation to the DBM transport presented in the current paper.

The outcomes of our study give rise to additional avenues for future research. From a theoretical perspective, our initial analysis falls short of establishing the convergence in KL divergence of the IDBM procedure to the solution to  $(S_{\text{dyn}})$ . The numerical and analytical results of Section 5.1 support that, under mild conditions, this stronger form of convergence is achieved. Non-asymptotic results would be particularly valuable, as they could elucidate the conditions under which either the IPF or IDBM methods are more favorable. Moreover, it would be desirable to introduce more easily verifiable conditions guaranteeing convergence of the IDBM procedure. Finally, when  $d > 1$ , neither the IPF nor the IDBM procedures are robust to vanishing randomness in the reference diffusion  $R$ . Consequently, the design of an iterative procedure solving  $(S_{\text{dyn}})$ , while being robust to a vanishing regularization level, remains an open problem.

On the empirical side, computational constraints limited the scope of our numerical comparison between the DBM transport and the time-reversal approach of Song et al. (2021). Specifically, no hyperparameter optimization was performed, neither for DBM-specific parameters nor for the employed neural network architecture, while Figure 6 suggests that the

tested configuration might suffer from overfitting later in training. This is conceivable, as the DBM transport approximates the solution to  $(S_{\text{dyn}})$ , which is associated to a SDE with a “simpler” optimal drift (Dai Pra, 1991). Since the exact solution to the DBM transport, and of the competing approaches, perfectly recovers the training data distribution, a less powerful architecture might be required for superior generalization properties. Overfitting to the CIFAR-10 dataset is not a novel concern (Nichol and Dhariwal, 2021), and it is typically addressed through hyperparameter search.

At one extreme, when the reference process’s dynamics imply a terminal value almost independent of the initial value, the DBM results in a generative model akin to that of Song et al. (2021), while rectifying the terminal distribution mismatch inherent in all time-reversal approaches (Bortoli et al., 2021). More generally, the DBM transport enlarges the space of feasible (exact) transports. Consequently, it is plausible that improvements in current state-of-the-art solutions can be attained by empirically exploring this enlarged space, optimizing for a given metric of interest, such as FID. In particular, higher-resolution images pose challenges for time-reversal approaches and necessitate an increase in the reference process randomness, thus increasing the implicit integration time (Hoogeboom et al., 2023). The DBM transport, which precisely matches the initial and terminal marginal distributions, does not face this issue. Lastly, computational constraints precluded an evaluation of the application of further iterations of the IDBM transport, which would trade off increased training time with a more efficient generation process.

# Appendices

## A Proofs

### Proof of Theorem 1

The following assumptions are sufficient for the application of Theorem 1. We assume that (21) and each member of (19) admits a unique solution, with strictly positive marginal densities over<sup>7</sup>  $\mathbb{R}^d$ . We assume that each marginal density is the unique solution to the corresponding Fokker-Plank PDE, and that the exchanges of limits denoted with  $(\star\star)$  hold.

When Theorem 1 is applied to construct  $\Pi = CR_{\bullet|0,\tau}$  in Section 3.4, these conditions are satisfied if  $R$  is given by (31) and the marginals of  $C$  are given by (finite) mixtures of Gaussian distributions. This covers the setting of generative modelling applications described in Section 2.5.

**Theorem 1** (Diffusion mixture matching). *Consider the family of  $d$ -dimensional SDEs indexed by  $\lambda \in \Lambda$*

$$\begin{aligned} dX_t^\lambda &= \mu^\lambda(X_t^\lambda, t)dt + g^\lambda(X_t^\lambda, t)dW_t^\lambda, \quad t \in [0, \tau], \\ X_0^\lambda &\sim P_0^\lambda, \end{aligned} \quad (19)$$

corresponding to the family of path PMs  $\{P^\lambda\}_{\lambda \in \Lambda}$ . For a mixing PM  $\Psi$  on  $\Lambda$ , let  $\Pi \in \mathcal{P}_C$  be obtained by taking the  $\Psi$ -mixture of (19) over  $\lambda \in \Lambda$ . In particular, define the mixture marginal densities  $\pi_t$ ,  $t \in (0, \tau)$ , and the mixture initial PM  $\Pi_0$  by

$$\pi_t(x) := \int_{\Lambda} p_t^\lambda(x) \Psi(d\lambda), \quad \Pi_0(dx) := \int_{\Lambda} P_0^\lambda(dx) \Psi(d\lambda). \quad (20)$$

Consider the  $d$ -dimensional SDE

$$\begin{aligned} dX_t &= \mu(X_t, t)dt + \sigma(X_t, t)dW_t, \quad t \in [0, \tau], \\ \mu(x, t) &:= \frac{\int_{\Lambda} \mu^\lambda(x, t) p_t^\lambda(x) \Psi(d\lambda)}{\pi_t(x)}, \\ \sigma(x, t) &:= \frac{\int_{\Lambda} g^\lambda(x, t) p_t^\lambda(x) \Psi(d\lambda)}{\pi_t(x)}, \\ Y_0 &\sim \Pi_0, \end{aligned} \quad (21)$$

with law  $P$ . Then, under mild conditions, for all  $t \in [0, \tau]$  it holds that  $P_t = \Pi_t$ .

*Proof.* In this proof we make use of the following notation: for  $f(x, t) : \mathbb{R}^d \times [0, \tau] \rightarrow \mathbb{R}$ ,  $(f(x, t))_t := \frac{d}{dt} f(x, t)$ , for  $f(x, t) : \mathbb{R}^d \times [0, \tau] \rightarrow \mathbb{R}^d$ ,  $(f(x, t))_x := \sum_{i=1}^d \frac{d}{dx_i} f(x, t)$ , for  $f(x, t) : \mathbb{R}^d \times [0, \tau] \rightarrow \mathbb{R}^d \times \mathbb{R}^d$ ,  $(f(x, t))_{xx} := \sum_{i,j=1}^d \frac{d^2}{dx_i dx_j} f(x, t)$ . Let  $G^\lambda(x, t) := g^\lambda(x, t)g^\lambda(x, t)^\top$ . Then, for  $0 < t \leq \tau$ ,

$$\begin{aligned} (\pi_t(x))_t &= \left( \int_{\Lambda} p_t^\lambda(x) \Psi(d\lambda) \right)_t \\ &= \int_{\Lambda} \left( p_t^\lambda(x) \right)_t \Psi(d\lambda) \end{aligned} \quad (\star\star)$$

---

<sup>7</sup>We do not consider the case of SDEs on constrained state-spaces.

$$\begin{aligned}
&= \int_{\Lambda} \left( \mu^{\lambda}(x, t) p_t^{\lambda}(x) \right)_x + \frac{1}{2} \left( G^{\lambda}(x, t) p_t^{\lambda}(x) \right)_{xx} \Psi(d\lambda) \\
&= \int_{\Lambda} \left( \frac{\mu^{\lambda}(x, t) p_t^{\lambda}(x)}{\pi_t(x)} \pi_t(x) \right)_x + \frac{1}{2} \left( \frac{G^{\lambda}(x, t) p_t^{\lambda}(x)}{\pi_t(x)} \pi_t(x) \right)_{xx} \Psi(d\lambda) \\
&= \left( \int_{\Lambda} \frac{\mu^{\lambda}(x, t) p_t^{\lambda}(x)}{\pi_t(x)} \Psi(d\lambda) \pi_t(x) \right)_x + \frac{1}{2} \left( \int_{\Lambda} \frac{G^{\lambda}(x, t) p_t^{\lambda}(x)}{\pi_t(x)} \Psi(d\lambda) \pi_t(x) \right)_{xx}. \quad (\star\star)
\end{aligned}$$

The lines denoted with  $(\star\star)$  consist of exchange of limits, the third line results from the application of the Fokker-Plank PDEs for  $\{P^{\lambda}\}_{\lambda \in \Lambda}$ . The Fokker-Plank PDE for (21) is

$$(p_t(x))_t = \left( \int_{\Lambda} \frac{\mu^{\lambda}(x, t) p_t^{\lambda}(x)}{\pi_t(x)} \Psi(d\lambda) p_t(x) \right)_x + \frac{1}{2} \left( \int_{\Lambda} \frac{G^{\lambda}(x, t) p_t^{\lambda}(x)}{\pi_t(x)} \Psi(d\lambda) p_t(x) \right)_{xx}.$$

As  $P_0 = \Pi_0$  and  $p$  and  $\pi$  satisfy the same Fokker-Plank PDE, it follows that  $P$  and  $\Pi$  share the same marginal distribution.  $\square$

## Proof of Theorem 2

**Theorem 2** (IDBM convergence). *For  $\Gamma, \Upsilon \in \mathcal{P}_1$ ,  $R \in \mathcal{P}_{\mathcal{C}}$  solution to (3) with  $\sigma_R(x, t) = I$ , consider the iterates  $\Pi^{(i)}, M^{(i)} \in \mathcal{P}_{\mathcal{C}}(\Gamma, \Upsilon)$  of Algorithm 2. Assume that<sup>8</sup>: (i)  $D_{KL}(C^{(0)} \parallel S_{0, \tau}^*) < \infty$ ; (ii) for each  $i \geq 0$  the Cameron-Martin-Girsanov theorem hold for  $M^{(i)}$  yielding  $dM^{(i)}/dS^*$  (implying that (22) for  $\Pi = \Pi^{(i)}$  has a unique diffusion solution with law  $M^{(i)}$ , and that  $M^{(i)} \ll S^*$ ). Then: (i)  $\Pi^{(i)} \xrightarrow{\mathcal{L}} S^*$  and  $M^{(i)} \xrightarrow{\mathcal{L}} S^*$  as  $i \rightarrow \infty$ , where  $\xrightarrow{\mathcal{L}}$  denotes converge in law; (ii)  $D_{KL}(\Pi^{(i)} \parallel S^*) \geq D_{KL}(M^{(i)} \parallel S^*) \geq D_{KL}(\Pi^{(i+1)} \parallel S^*)$  for  $i \geq 0$  (implying that  $D_{KL}(M^{(i)} \parallel S^*)$  is non-increasing in  $i$ ); (iii)  $D_{KL}(\Pi(C) \parallel S^*) = D_{KL}(M(C) \parallel S^*)$  if and only if  $\Pi(C) = M(C) = S^*$ .*

*Proof.* Let  $P \in \mathcal{P}_{\mathcal{C}}$  be the law of the diffusion solving

$$\begin{aligned}
dX_t &= \mu(X_t, t)dt + \sigma_R(X_t, t)dW_t, \quad t \in [0, \tau], \\
X_0 &\sim P_0.
\end{aligned}$$

Let  $C \in \mathcal{P}_2(\Gamma, \Upsilon)$ . Within this proof, we use the following abbreviations:  $\Pi(C) := \Pi(C, R_{\bullet|0, \tau})$ ,  $M(C) := M(\Pi(C, R_{\bullet|0, \tau}))$ ,  $S^* := S^*(\Gamma, \Upsilon, R, \mathcal{P}_{\mathcal{C}})$ . Assume that  $D_{KL}(\Pi(C) \parallel P) < \infty$  and that the conditions required for the application of the Cameron-Martin-Girsanov theorem to obtain  $dM(C)/dP$  are satisfied. As  $M(C) \ll P$  as well, following Csiszar (1975), it holds that

$$\begin{aligned}
D_{KL}(\Pi(C) \parallel P) - D_{KL}(\Pi(C) \parallel M(C)) &= \mathbb{E}_{\Pi(C)} \left[ \log \frac{d\Pi(C)}{dP} \right] - \mathbb{E}_{\Pi(C)} \left[ \log \frac{d\Pi(C)}{dM(C)} \right] \\
&= \mathbb{E}_{\Pi(C)} \left[ \log \frac{dM(C)}{dP} \right],
\end{aligned}$$

and we want to show that

$$\mathbb{E}_{\Pi(C)} \left[ \log \frac{dM(C)}{dP} \right] = \mathbb{E}_{M(C)} \left[ \log \frac{dM(C)}{dP} \right].$$

As  $\Pi_0(C) = M_0(C) = \Gamma$  it suffices to show that

$$\mathbb{E}_{\Pi(C)} \left[ \log \frac{dM_{\bullet|0}(C)}{dP_{\bullet|0}} \right] = \mathbb{E}_{M(C)} \left[ \log \frac{dM_{\bullet|0}(C)}{dP_{\bullet|0}} \right],$$

<sup>8</sup>As in the proof, we denote  $\Pi(C) := \Pi(C, R_{\bullet|0, \tau})$ ,  $M(C) := M(\Pi(C, R_{\bullet|0, \tau}))$ ,  $S^* := S^*(\Gamma, \Upsilon, R, \mathcal{P}_{\mathcal{C}})$ .

where

$$\log \frac{dM_{\bullet|0}(C)}{dP_{\bullet|0}}(x) = \int_0^\tau [(\mu_M - \mu)^\top \Sigma_R^{-1}](x_t, t) dx_t - \frac{1}{2} \int_0^\tau [(\mu_M - \mu)^\top \Sigma_R^{-1}(\mu_M + \mu)](x_t, t) dt$$

is given by (11). As  $\Pi(\delta_{x_0} \otimes \Upsilon, R_{\bullet|0, \tau}) = \Pi_{\bullet|0}(C, R_{\bullet|0, \tau})$ , from (23),

$$\begin{aligned} & \mathbb{E}_{\Pi(C)} \left[ \int_0^\tau [(\mu_M - \mu)^\top \Sigma_R^{-1}](X_t, t) dX_t \right] \\ &= \mathbb{E}_{\Pi(C)} \left[ \int_0^\tau [(\mu_M - \mu)^\top \Sigma_R^{-1}](X_t, t) (\mu_R(X_t, t) + \Sigma_R(X_t, t) \mathbb{E}_{\Pi(C)} [\nabla_{X_t} \log r_{\tau|t}(X_\tau | X_t) | X_t, X_0]) dt \right] \\ &= \mathbb{E}_{\Pi(C)} \left[ \int_0^\tau [(\mu_M - \mu)^\top \Sigma_R^{-1}](X_t, t) (\mu_R(X_t, t) + \Sigma_R(X_t, t) \mathbb{E}_{\Pi(C)} [\nabla_{X_t} \log r_{\tau|t}(X_\tau | X_t) | X_t]) dt \right], \end{aligned}$$

by the tower property of conditional expectations. On the other hand, from (22),

$$\begin{aligned} & \mathbb{E}_{M(C)} \left[ \int_0^\tau [(\mu_M - \mu)^\top \Sigma_R^{-1}](X_t, t) dX_t \right] \\ &= \mathbb{E}_{M(C)} \left[ \int_0^\tau [(\mu_M - \mu)^\top \Sigma_R^{-1}](X_t, t) (\mu_R(X_t, t) + \Sigma_R(X_t, t) \mathbb{E}_{\Pi(C)} [\nabla_{X_t} \log r_{\tau|t}(X_\tau | X_t) | X_t]) dt \right] \\ &= \mathbb{E}_{\Pi(C)} \left[ \int_0^\tau [(\mu_M - \mu)^\top \Sigma_R^{-1}](X_t, t) (\mu_R(X_t, t) + \Sigma_R(X_t, t) \mathbb{E}_{\Pi(C)} [\nabla_{X_t} \log r_{\tau|t}(X_\tau | X_t) | X_t]) dt \right], \end{aligned}$$

as  $M_t(C) = \Pi_t(C)$  for all  $t \in [0, \tau]$ . In the same way, equality in expectations of  $-\frac{1}{2} \int_0^\tau [(\mu_M - \mu)^\top \Sigma_R^{-1}(\mu_M + \mu)](X_t, t) dt$  is established. We thus obtain a version of the Pythagorean law for (reverse) KL-projections (Csiszar, 1975; Nielsen, 2018),

$$D_{KL}(\Pi(C) \| P) = D_{KL}(\Pi(C) \| M(C)) + D_{KL}(M(C) \| P).$$

See also Liu et al. (2023) for another derivation of this result. When  $P = S^*$  ( $S^*$  is law of the diffusion solving (18)), under the same assumptions,

$$D_{KL}(\Pi(C) \| S^*) \geq D_{KL}(M(C) \| S^*), \quad (40)$$

with equality if and only if  $\Pi(C) = M(C)$ .

If  $\Pi(C) = S^*$ , then  $M(C) = S^*$  as  $\Pi(C) = CR_{\bullet|0, \tau}$  is equal in law to the diffusion process solving (18) and Theorem 1 applied to a (single) diffusion results in that same diffusion. On the other hand, if  $\Pi(C) \neq S^*$ , then  $\Pi(C)$  is not a diffusion (it is an Ito process in the sense of Øksendal (2003)), see Section 3.2, and  $M(C) \neq \Pi(C)$  (Øksendal, 2003, Theorem 8.4.3). That is  $\Pi(C) = M(C)$  if and only if  $\Pi(C) = M(C) = S^*$ .

For  $i \geq 0$ ,

$$\begin{aligned} D_{KL}(\Pi^{(i)} \| S^*) &= D_{KL}(\Pi_{0, \tau}^{(i)} \| S_{0, \tau}^*) + \mathbb{E}_{\Pi_{0, \tau}^{(i)}} [D_{KL}(\Pi_{\bullet|0, \tau}^{(i)} \| S_{\bullet|0, \tau}^*)] \\ &= D_{KL}(\Pi_{0, \tau}^{(i)} \| S_{0, \tau}^*), \end{aligned}$$

as  $\Pi_{\bullet|0, \tau}^{(i)} = S_{\bullet|0, \tau}^* = R_{\bullet|0, \tau}$ , and

$$\begin{aligned} D_{KL}(M^{(i)} \| S^*) &= D_{KL}(M_{0, \tau}^{(i)} \| S_{0, \tau}^*) + \mathbb{E}_{M_{0, \tau}^{(i)}} [D_{KL}(M_{\bullet|0, \tau}^{(i)} \| S_{\bullet|0, \tau}^*)] \\ &\geq D_{KL}(\Pi_{0, \tau}^{(i+1)} \| S_{0, \tau}^*), \end{aligned}$$

as  $M_{0,\tau}^{(i)} = \Pi_{0,\tau}^{(i+1)}$ . Thus,

$$D_{KL}(M^{(i)} \parallel S^*) \geq D_{KL}(\Pi^{(i+1)} \parallel S^*). \quad (41)$$

It is assumed that  $D_{KL}(\Pi^{(0)} \parallel S^*) = D_{KL}(C^{(0)} \parallel S_{0,\tau}^*) < \infty$ , and that the Cameron-Martin-Girsanov theorem applies to each  $M^{(i)}$  yielding  $dM^{(i)}/dS^*$ . Therefore, we can iteratively apply (40) and (41) obtaining  $D_{KL}(\Pi^{(i)} \parallel S^*) \geq D_{KL}(M^{(i)} \parallel S^*) \geq D_{KL}(\Pi^{(i+1)} \parallel S^*)$  for  $i \geq 0$ . Being non-increasing and bounded below, the sequence  $D_{KL}(\Pi^{(i)} \parallel S^*), D_{KL}(M^{(i)} \parallel S^*), D_{KL}(\Pi^{(i+1)} \parallel S^*)$  converges, and  $\lim_{i \rightarrow \infty} (D_{KL}(\Pi^{(i)} \parallel S^*) - D_{KL}(M^{(i)} \parallel S^*)) = \lim_{i \rightarrow \infty} D_{KL}(\Pi^{(i)} \parallel M^i) = 0$ .

The sequences  $\{\Pi^{(i)}\}_{i \geq 0}$ ,  $\{M^{(i)}\}_{i \geq 0}$  are tight. We consider  $\{\Pi^{(i)}\}_{i \geq 0}$ , the case of  $\{M^{(i)}\}_{i \geq 0}$  being identical. By the conditional Jensen inequality, for any measurable set  $K$ ,

$$\begin{aligned} D_{KL}(\Pi^{(i)} \parallel S^*) &= \mathbb{E}_{\Pi^{(i)}} \left[ -\log \frac{dS^*}{d\Pi^{(i)}} \Big| K^c \right] \Pi^{(i)}[K^c] + \mathbb{E}_{\Pi^{(i)}} \left[ -\log \frac{dS^*}{d\Pi^{(i)}} \Big| K \right] \Pi^{(i)}[K] \\ &\geq -\log(S^*[K^c]/\Pi^{(i)}[K^c])\Pi^{(i)}[K^c] + -\log(S^*[K]/\Pi^{(i)}[K])\Pi^{(i)}[K]. \end{aligned}$$

For  $\varepsilon > 0$ , choose  $K$  compact such  $S^*[K^c] < \varepsilon$ ,  $S^*[K] \geq 1 - \varepsilon$  by the tightness of  $S^*$  (as it is defined on a Polish space, see Léonard (2014a)). Assume that  $\Pi^{(i)}$  is not tight. That is, there is  $\gamma > 0$  such that for each compact  $K$  there is  $i \geq 0$  with  $\Pi^{(i)}[K^c] \geq \gamma$ ,  $\Pi^{(i)}[K] < 1 - \gamma$ . Hence, for each  $\varepsilon > 0$ , there is  $i \geq 0$  such that

$$-\log(S^*[K^c]/\Pi^{(i)}[K^c])\Pi^{(i)}[K^c] \geq -\log(\varepsilon/\gamma)\gamma,$$

which can be made arbitrarily large by a suitable small  $\varepsilon > 0$ . On the other hand,  $-\log(S^*[K]/x)x$  is bounded below for  $x \in [0, 1]$ , so  $-\log(S^*[K]/\Pi^{(i)}[K])\Pi^{(i)}[K]$  is bounded below. But we know that for  $i$  large enough  $D_{KL}(\Pi^{(i)} \parallel S^*)$  is bounded above, hence  $\Pi^{(i)}$  must be tight.

Therefore,  $\{\Pi^{(i)}\}_{i \geq 0}$  and  $\{M^{(i)}\}_{i \geq 0}$  are relatively compact. Each subsequence of  $\{\Pi^{(i)}\}_{i \geq 0}$  has a further subsequence  $\{\Pi^{(l)}\}_{l \geq 1}$  which converges in law:  $\Pi^{(l)} \xrightarrow{\mathcal{L}} \Pi^{(\infty)}$  as  $l \rightarrow \infty$  for some  $\Pi^{(\infty)} \in \mathcal{P}_{\mathcal{C}}(\Gamma, \Upsilon)$ . Each subsequence of  $\{M^{(i)}\}_{i \geq 0}$  has a further subsequence  $\{M^{(l)}\}_{l \geq 1}$  which converges in law:  $M^{(l)} \xrightarrow{\mathcal{L}} M^{(\infty)}$  for some  $M^{(\infty)} \in \mathcal{P}_{\mathcal{C}}(\Gamma, \Upsilon)$ . By the lower semi-continuity of the KL divergence with respect to the topology of weak convergence (van Erven and Harremos, 2014, Theorem 19),  $0 = \liminf_{l \rightarrow \infty} D_{KL}(\Pi^{(l)} \parallel M^l) \geq D_{KL}(\Pi^{(\infty)} \parallel M^{(\infty)})$  and therefore  $\Pi^{(\infty)} = M^{(\infty)}$ . Denote this common PM with  $S^{(\infty)}$ .

Due to the convergence in law of  $\Pi^{(l)}$ , and the form of its disintegration,  $S^{(\infty)}$  is of the form  $S_{0,\tau}^{(\infty)} R_{\bullet|0,\tau}$  for some  $S_{0,\tau}^{(\infty)} \in \mathcal{P}_2(\Gamma, \Upsilon)$ . If  $S^{(\infty)}$  is also diffusion, it follows that  $S_{0,\tau}^{(\infty)} = S_{0,\tau}^{(*)}$  (Section 3.2) and thus  $S^{(\infty)} = S^*$ . It remains to show that  $S^{(\infty)}$  is a diffusion when  $\sigma_R(x, t) = I$ . Again by the lower semi-continuity of the KL divergence, we have that  $D_{KL}(S^{(\infty)} \parallel S^*) < \infty$  and thus  $S^{(\infty)} \ll S^*$ . But  $S^* \ll R$  and  $R \ll R^\circ$  by assumption where  $R^\circ$  is the  $d$ -dimensional Brownian measure on  $[0, \tau]$ . Then, by Liptser and Shiriaev (1977, Theorem 7.11 and following Note 1),  $S^{(\infty)}$  is a diffusion.

As convergence in law to  $S^*$  has been established for arbitrary convergent subsequences,  $\{\Pi^{(i)}\} \xrightarrow{\mathcal{L}} S^{(\infty)}$  and  $\{M^{(i)}\} \xrightarrow{\mathcal{L}} S^{(\infty)}$  by Billingsley (1999, Theorem 2.6).  $\square$

## B SDE Class

The linearity of (28) and (29) stands behind the form of the conditional expectations entering the drift coefficients that follow. The generative time reversal process (15) is given by

$$d\bar{X}_t = \left[ \alpha\beta_\tau\bar{X}_t + \beta_\tau \frac{\mathbb{E}_R[\bar{X}_\tau|\bar{X}_t]a(0, b_\tau) - \bar{X}_t}{v(0, b_\tau)} \right] dt + \sqrt{\beta_\tau}\Gamma^{1/2}dW_t, \quad t \in [0, \tau],$$

$$\bar{X}_0 \sim R_\tau \approx \Upsilon,$$

the DBM transport (22) is given by

$$dX_t = \left[ -\alpha\beta_t X_t + \beta_t \frac{\mathbb{E}_\Pi[X_\tau|X_t]a(b_t, b_\tau) - X_t a(b_t, b_\tau)^2}{v(b_t, b_\tau)} \right] dt + \sqrt{\beta_t}\Gamma^{1/2}dW_t, \quad t \in [0, \tau],$$

$$X_0 \sim \Gamma,$$

while the BDBM transport (24) is given by

$$d\bar{X}_t = \left[ \alpha\beta_t\bar{X}_t + \beta_t \frac{\mathbb{E}_\Pi[\bar{X}_\tau|\bar{X}_t]a(0, b_\tau) - \bar{X}_t}{v(0, b_\tau)} \right] dt + \sqrt{\beta_t}\Gamma^{1/2}dW_t, \quad t \in [0, \tau],$$

$$\bar{X}_0 \sim \Upsilon.$$

For  $\alpha = 0$ , the DBM and BDBM transports are symmetric in the following sense: the BDM transport based on  $C \in \mathcal{P}_2(\Gamma, \Upsilon)$  and  $\beta_t$  is equivalent in law to the BDBM transport based on  $\bar{C} \in \mathcal{P}_2(\Upsilon, \Gamma)$  and  $\bar{\beta}_t := \beta_\tau$ .

## C Score Generative

---

```

1 # requires:
2 #   b_t(t): b_t(t)
3 #   a_s_t(s, t): a(s, t) from (29)
4 #   v_s_t(s, t): v(s, t) from (29)
5 # inputs:
6 #   x_0: [B, C, H, W]
7 #   model: ([B, C, H, W], [B]) -> [B, C, H, W]
8 # outputs:
9 #   losses: [B]
10 def sgm_loss(x_0, model, T=1.0):
11     t = torch.rand(x_0.shape[0], device=x_0.device) * T # [B]
12     scaled_t = b_t(t) # [B]
13     z = torch.randn_like(x_0) # [B, C, H, W]
14     a_0_t, v_0_t = a_s_t(0.0, scaled_t), v_s_t(0.0, scaled_t) # [B]
15     s_0_t = torch.sqrt(v_0_t) # [B]
16     x_t = a_0_t[:, None, None, None] * x_0 + s_0_t[:, None, None, None] * z # [B, C, H, W]
17     score_t = (x_0 * a_0_t[:, None, None, None] - x_t) / v_0_t[:, None, None, None] # [B, C, H, W]
18     losses = (model(x_t, scaled_t) - score_t)**2 * v_0_t[:, None, None, None] # [B, C, H, W]
19     losses = torch.sum(losses.view(losses.shape[0], -1), dim=1) # [B]
20     return losses

```

---

Listing 1: SGM loss sampling;  $\mathbf{x}_0$  is a batch of  $B$  images, each of which has  $C$  channels, height  $H$  and width  $W$ .

---

```

1 # requires:
2 #     b_t(t):  $b_t(t)$ 
3 #     a_s_t(s, t):  $a(s, t)$  from (29)
4 #     v_s_t(s, t):  $v(s, t)$  from (29)
5 #     al_s_t_u(s, t, u):  $\hat{a}(s, t, u)$  from (32)
6 #     ar_s_t_u(s, t, u):  $\hat{a}(s, t, u)$  from (32)
7 #     vb_s_t_u(s, t, u):  $\tilde{v}(s, t, u)$  from (32)
8 # inputs:
9 #     x_0: [B, C, H, W]
10 #     model: ([B, C, H, W], [B]) -> [B, C, H, W]
11 # outputs:
12 #     losses: [B]
13 def bdbm_loss(x_0, model, T=1.0, sigma_T=1.0):
14     t = torch.rand(x_0.shape[0], device=x_0.device) * T # [B]
15     scaled_t, scaled_T = b_t(t), b_t(T) # [B]
16     z = torch.randn_like(x_0) # [B, C, H, W]
17     a_0_t, v_0_t = a_s_t(0.0, scaled_t), v_s_t(0.0, scaled_t) # [B]
18     x_T = torch.randn_like(x_0) * sigma_T # [B, C, H, W]
19     al_0_t_T, ar_0_t_T, = al_s_t_u(0.0, t, scaled_T), ar_s_t_u(0.0, t, scaled_T) # [B]
20     vb_0_t_T = vb_s_t_u(0.0, t, scaled_T) # [B]
21     sb_0_t_T = torch.sqrt(vb_0_t_T) # [B]
22     x_t = (
23         + al_0_t_T[:, None, None, None] * x_0
24         + ar_0_t_T[:, None, None, None] * x_T
25         + sb_0_t_T[:, None, None, None] * z
26     ) # [B, C, H, W]
27     score_t = (x_0 * a_0_t[:, None, None, None] - x_t) / v_0_t[:, None, None, None] # [B, C, H, W]
28     losses = (model(x_t, scaled_t) - score_t)**2 * v_0_t[:, None, None, None] # [B, C, H, W]
29     losses = torch.sum(losses.view(losses.shape[0], -1), dim=1) # [B]
30     return losses

```

---

Listing 2: BDBM loss sampling;  $x_0$  is a batch of  $B$  images, each of which has  $C$  channels, height  $H$  and width  $W$ .

## D Notation

Notation	Description
$[0, \tau]$	Time interval
$d$	Dimension of state space
$P, Q, \dots$	Probability measure (PM)
$\mathcal{P}_C$	PMs over $\mathcal{C}([0, \tau], \mathbb{R}^d)$
$\mathcal{P}_n$	PMs over $\mathbb{R}^{d \times n}$
$\mathcal{P}_C(\Gamma, \Upsilon)$	PMs with initial-terminal distributions $\Gamma, \Upsilon$ ; $\mathcal{P}_C(\Gamma, \Upsilon) \subseteq \mathcal{P}_C$
$\mathcal{P}_2(\Gamma, \Upsilon)$	PMs with marginal distributions $\Gamma, \Upsilon$ ; $\mathcal{P}_2(\Gamma, \Upsilon) \subseteq \mathcal{P}_2$
$\mathcal{U}(0, \tau)$	Uniform distribution on $(0, \tau)$
$\mathcal{N}_d(\mu, \Sigma)$	$d$ -variate normal distribution with mean $\mu$ and covariance $\Sigma$
$dP/dQ$	Density of PM $P$ with respect to PM $Q$
$p$	Lebesgue density of PM $P$
$P_{t_1, \dots, t_n}$	Marginalization of $P \in \mathcal{P}_C$ at $t_1, \dots, t_n$
$P_{\bullet t_1, \dots, t_n}$	Conditioning of $P \in \mathcal{P}_C$ given values at $t_1, \dots, t_n$
$P = P_{t_1, \dots, t_n} P_{\bullet t_1, \dots, t_n}$	Marginal-conditional decomposition of $P \in \mathcal{P}_C$
$Q = \Psi P_{\bullet t_1, \dots, t_n}$	Mixing of $P \in \mathcal{P}_C$ via $\Psi \in \mathcal{P}_n$ at times $t_1, \dots, t_n$ ; $Q \in \mathcal{P}_C$
$D_{KL}(S \parallel R)$	Kullback-Leibler divergence from PM $S$ to PM $R$
$I$	Identity matrix
$A^\top$	Transposition of a square matrix $A$
$\ V\ $	Euclidean norm of a vector $V$
$\bar{X}$	Time reversal of stochastic process $X$
$\bar{P}$	Time reversal of PM $P$ ; $P \in \mathcal{P}_C$
$\mathfrak{r}$	Reverse timescale; $\mathfrak{r} := \tau - t$
$W$	$d$ -dimensional standard Brownian motion
$\Gamma, \Upsilon$	Target PMs; $\Gamma, \Upsilon \in \mathcal{P}_1$
$R$	Reference PM; $R \in \mathcal{P}_C$
$\mu_R(x, t), \sigma_R(x, t)$	Reference SDE drift and diffusion coefficients
$\Sigma_R(x, t)$	Reference SDE covariance coefficient; $\Sigma_R := \sigma_R \sigma_R^\top$
$S^*(\Gamma, \Upsilon, R, \mathcal{P}_C)$	Solution ( $S_{\text{dyn}}$ ) (dynamic)
$S^*(\Gamma, \Upsilon, R_{0, \tau}, \mathcal{P}_2)$	Solution to ( $S_{\text{sta}}$ ) (static) (corresponding to ( $S_{\text{dyn}}$ ))
$S^*(\Gamma, \cdot, Q, \mathcal{P})$	Solution to forward ( $H_{\text{dyn}}$ ) ( $\mathcal{P} = \mathcal{P}_C$ ), ( $H_{\text{sta}}$ ) ( $\mathcal{P} = \mathcal{P}_2$ ); $Q \in \mathcal{P}$
$S^*(\cdot, \Upsilon, Q, \mathcal{P})$	Solution to backward ( $H_{\text{dyn}}$ ) ( $\mathcal{P} = \mathcal{P}_C$ ), ( $H_{\text{sta}}$ ) ( $\mathcal{P} = \mathcal{P}_2$ ); $Q \in \mathcal{P}$
$F^{(i)}$	$i$ -th IPF iteration; $F^{(i)} \in \mathcal{P}_C \cup \mathcal{P}_2, i \geq 0$
$\mu_{F^{(i)}}$	Drift corresponding to $F^{(i)} \in \mathcal{P}_C$
$\Pi(C, R_{\bullet 0, \tau})$	Diffusion mixture; $C \in \mathcal{P}_2(\Gamma, \Upsilon), \Pi \in \mathcal{P}_C(\Gamma, \Upsilon)$
$M(\Pi(C, R_{\bullet 0, \tau}))$	Forward IDBM based on $C$ ; $C \in \mathcal{P}_2(\Gamma, \Upsilon), M \in \mathcal{P}_C(\Gamma, \Upsilon)$
$\bar{M}(\Pi(C, R_{\bullet 0, \tau}))$	Backward IDBM based on $C$ ; $C \in \mathcal{P}_2(\Gamma, \Upsilon), \bar{M} \in \mathcal{P}_C(\Upsilon, \Gamma)$
$M^{(i)}$	$i$ -th (forward) IDBM iteration; $M^{(i)} \in \mathcal{P}_C, i \geq 0$
$C^{(i)}$	$i$ -th IDBM coupling; $C^{(i)} \in \mathcal{P}_2(\Gamma, \Upsilon), C^{(i)} := M_{0, \tau}^{(i-1)} (C^{(0)} := \Gamma \otimes \Upsilon)$
$\Pi^{(i)}$	$i$ -th IDBM diffusion mixture; $\Pi^{(i)} \in \mathcal{P}_C, \Pi^{(i)} := \Pi(C^{(i)}, R_{\bullet 0, \tau})$
$\mu_{M^{(i)}}$	Drift corresponding to the $i$ -th IDBM iteration

Table 2: Main notation summary.

## References

- Anderson, B. D. (1982). Reverse-Time Diffusion Equation Models. *Stochastic Processes and their Applications*, 12(3):313–326.
- Bernton, E., Heng, J., Doucet, A., and Jacob, P. E. (2019). Schrödinger Bridge Samplers.
- Billingsley, P. (1999). *Convergence of Probability Measures*. Wiley Series in Probability and Statistics. Probability and Statistics Section. Wiley, 2nd ed edition.
- Bortoli, V. D., Thornton, J., Heng, J., and Doucet, A. (2021). Diffusion Schrödinger Bridge with Applications to Score-Based Generative Modeling. In *Thirty-Fifth Conference on Neural Information Processing Systems*.
- Brigo, D. (2002). The General Mixture-Diffusion SDE and Its Relationship with an Uncertain-Volatility Option Model with Volatility-Asset Decorrelation.
- Brooks, S., Gelman, A., Jones, G., and Meng, X.-L. (2011). *Handbook of Markov Chain Monte Carlo*. CRC press.
- Csiszar, I. (1975). I-Divergence Geometry of Probability Distributions and Minimization Problems. *The Annals of Probability*, 3(1):146–158.
- Dai Pra, P. (1991). A stochastic control approach to reciprocal diffusion processes. *Applied Mathematics and Optimization*, 23(1):313–329.
- Deming, W. E. and Stephan, F. F. (1940). On a Least Squares Adjustment of a Sampled Frequency Table When the Expected Marginal Totals are Known. *The Annals of Mathematical Statistics*, 11(4):427–444.
- Dvurechensky, P., Gasnikov, A., and Kroshnin, A. (2018). Computational Optimal Transport: Complexity by Accelerated Gradient Descent Is Better Than by Sinkhorn’s Algorithm. In *Proceedings of the 35th International Conference on Machine Learning*, pages 1367–1376. PMLR.
- El Moselhy, T. A. and Marzouk, Y. M. (2012). Bayesian inference with optimal maps. *Journal of Computational Physics*, 231(23):7815–7850.
- Flamary, R., Courty, N., Gramfort, A., Alaya, M. Z., Boisbunon, A., Chambon, S., Chapel, L., Corenflos, A., Fatras, K., Fournier, N., Gautheron, L., Gayraud, N. T. H., Janati, H., Rakotomamonjy, A., Redko, I., Rolet, A., Schutz, A., Seguy, V., Sutherland, D. J., Tavenard, R., Tong, A., and Vayer, T. (2021). POT: Python Optimal Transport. *Journal of Machine Learning Research*, 22(78):1–8.
- Fortet, R. (1940). Résolution d’un système d’équations de M. Schrödinger. *J. Math. Pure Appl. IX*, 1:83–105.
- Friedman, A. (1975). *Stochastic Differential Equations and Applications - Volume 1*. Probability and Mathematical Statistics Series ; v. 28. Academic Press.
- Fuchs, C. (2013). *Inference for Diffusion Processes: With Applications in Life Sciences*. Springer Science & Business Media.

- Haussmann, U. G. and Pardoux, E. (1986). Time Reversal of Diffusions. *The Annals of Probability*, 14(4):1188–1205.
- Heusel, M., Ramsauer, H., Unterthiner, T., Nessler, B., and Hochreiter, S. (2017). GANs Trained by a Two Time-Scale Update Rule Converge to a Local Nash Equilibrium. In *Advances in Neural Information Processing Systems*, volume 30. Curran Associates, Inc.
- Hoogeboom, E., Heek, J., and Salimans, T. (2023). Simple diffusion: End-to-end diffusion for high resolution images.
- Hurn, A. S., Jeisman, J. I., and Lindsay, K. A. (2007). Seeing the Wood for the Trees: A Critical Evaluation of Methods to Estimate the Parameters of Stochastic Differential Equations. *Journal of Financial Econometrics*, 5(3):390–455.
- Hyvärinen, A. (2005). Estimation of Non-Normalized Statistical Models by Score Matching. *Journal of Machine Learning Research*, 6(24):695–709.
- Jamison, B. (1974). Reciprocal processes. *Zeitschrift für Wahrscheinlichkeitstheorie und Verwandte Gebiete*, 30(1):65–86.
- Jamison, B. (1975). The Markov processes of Schrödinger. *Zeitschrift für Wahrscheinlichkeitstheorie und Verwandte Gebiete*, 32(4):323–331.
- Janati, H., Muzellec, B., Peyré, G., and Cuturi, M. (2020). Entropic Optimal Transport between Unbalanced Gaussian Measures has a Closed Form. In Larochelle, H., Ranzato, M., Hadsell, R., Balcan, M. F., and Lin, H., editors, *Advances in Neural Information Processing Systems*, volume 33, pages 10468–10479. Curran Associates, Inc.
- Kessler, M., Lindner, A., and Sorensen, M. (2012). *Statistical Methods for Stochastic Differential Equations*. Chapman and Hall/CRC.
- Kloeden, P. E. and Platen, E. (1992). *Numerical Solution of Stochastic Differential Equations*. Springer Berlin Heidelberg, Berlin, Heidelberg.
- Liptser, R. S. and Shiriaev, A. N. (1977). *Statistics of Random Processes: General Theory*, volume 394. Springer.
- Liu, Q. (2022). Rectified Flow: A Marginal Preserving Approach to Optimal Transport.
- Liu, X., Gong, C., and Liu, Q. (2022). Flow Straight and Fast: Learning to Generate and Transfer Data with Rectified Flow.
- Liu, X., Wu, L., Ye, M., and Liu, Q. (2023). Learning Diffusion Bridges on Constrained Domains. In *The Eleventh International Conference on Learning Representations*.
- Léonard, C. (2014a). Some Properties of Path Measures. In Donati-Martin, C., Lejay, A., and Rouault, A., editors, *Séminaire de Probabilités XLVI*, Lecture Notes in Mathematics, pages 207–230. Springer International Publishing.
- Léonard, C. (2014b). A survey of the Schrödinger problem and some of its connections with optimal transport. *Discrete & Continuous Dynamical Systems*, 34(4):1533.
- Mallasto, A., Gerolin, A., and Minh, H. Q. (2022). Entropy-regularized 2-Wasserstein distance between Gaussian measures. *Information Geometry*, 5(1):289–323.

- Marzouk, Y., Moselhy, T., Parno, M., and Spantini, A. (2016). Sampling via Measure Transport: An Introduction. In Ghanem, R., Higdon, D., and Owhadi, H., editors, *Handbook of Uncertainty Quantification*, pages 1–41. Springer International Publishing.
- Millet, A., Nualart, D., and Sanz, M. (1989). Integration by Parts and Time Reversal for Diffusion Processes. *The Annals of Probability*, pages 208–238.
- Nichol, A. Q. and Dhariwal, P. (2021). Improved Denoising Diffusion Probabilistic Models. In *Proceedings of the 38th International Conference on Machine Learning*, pages 8162–8171. PMLR.
- Nielsen, F. (2018). What is an information projection. *Notices of the AMS*, 65(3):321–324.
- Papamakarios, G., Nalisnick, E., Rezende, D. J., Mohamed, S., and Lakshminarayanan, B. (2021). Normalizing Flows for Probabilistic Modeling and Inference. *Journal of Machine Learning Research*, 22(57):1–64.
- Pavon, M., Tabak, E. G., and Trigila, G. (2018). The data-driven Schroedinger bridge.
- Peyré, G. and Cuturi, M. (2020). Computational Optimal Transport.
- Rogers, L. C. G. and Williams, D. (2000). *Diffusions, Markov Processes and Martingales: Volume 2: Itô Calculus*, volume 2. Cambridge university press.
- Rombach, R., Blattmann, A., Lorenz, D., Esser, P., and Ommer, B. (2022). High-Resolution Image Synthesis with Latent Diffusion Models. In *Proceedings of the IEEE Conference on Computer Vision and Pattern Recognition (CVPR)*.
- Ruschendorf, L. (1995). Convergence of the Iterative Proportional Fitting Procedure. *The Annals of Statistics*, 23(4):1160–1174.
- Rüschemdorf, L. and Thomsen, W. (1993). Note on the Schrödinger equation and I-projections. *Statistics & Probability Letters*, 17(5):369–375.
- Shi, Y., De Bortoli, V., Campbell, A., and Doucet, A. (2023). Diffusion Schrödinger Bridge Matching.
- Song, Y., Sohl-Dickstein, J., Kingma, D. P., Kumar, A., Ermon, S., and Poole, B. (2021). Score-Based Generative Modeling through Stochastic Differential Equations. In *International Conference on Learning Representations*.
- Stroock, D. W. and Varadhan, S. R. S. (2006). *Multidimensional Diffusion Processes*.
- Särkkä, S. and Solin, A. (2019). *Applied Stochastic Differential Equations*. Cambridge University Press, first edition.
- van Erven, T. and Harremoës, P. (2014). Rényi Divergence and Kullback-Leibler Divergence. *IEEE Transactions on Information Theory*, 60(7):3797–3820.
- Vargas, F., Thodoroff, P., Lamacraft, A., and Lawrence, N. (2021). Solving Schrödinger Bridges via Maximum Likelihood. *Entropy*, 23(9):1134.
- Vincent, P. (2011). A Connection Between Score Matching and Denoising Autoencoders. *Neural Computation*, 23(7):1661–1674.

- Wang, G., Jiao, Y., Xu, Q., Wang, Y., and Yang, C. (2021). Deep Generative Learning via Schrödinger Bridge. In Meila, M. and Zhang, T., editors, *Proceedings of the 38th International Conference on Machine Learning*, volume 139 of *Proceedings of Machine Learning Research*, pages 10794–10804. PMLR.
- Wu, L., Gong, C., Liu, X., Ye, M., and Liu, Q. (2022). Diffusion-based Molecule Generation with Informative Prior Bridges. In *Advances in Neural Information Processing Systems*.
- Øksendal, B. K. (2003). *Stochastic Differential Equations: An Introduction with Applications*. Universitext. Springer, Berlin ; New York, 6th ed. edition.